Int J Earth Sci (Geol Rundsch) (2017) 106:2297–2318
DOI 10.1007/s00531-016-1427-8

ORIGINAL PAPER

The role of precursory structures on Tertiary deformation in the Black Forest—Hegau region

Daniel Egli[1,2] · **Jon Mosar**[1] · **Tobias Ibele**[1,3] · **Herfried Madritsch**[4]

Received: 26 January 2016 / Accepted: 16 November 2016 / Published online: 8 December 2016

Abstract Structural inheritance of preexisting crustal discontinuities is widely accepted to have played a crucial role during the Cenozoic tectonic evolution of the northern Alpine foreland. It is recognised as a process that can strongly influence local fault kinematics and strain patterns. The case study presented herein is dedicated to the tectonic analysis of the Freiburg–Bonndorf–Bodensee Fault Zone (FBBFZ) located at the external margin of the northern Alpine Molasse Basin and extending into the crystalline Black Forest Massif. The structure and kinematics of this crustal-scale fault zone are investigated by means of a regional analysis of locally mapped faults, kinematic analysis of outcrop-scale fractures and slip vector modelling. The exceptional possibility of analysing the fault zone exposed from basement to cover allowed for an evaluation of interaction between precursory structures and subsequent deformation features. The results of this study show that the crystalline basement structures exposed along the FBBFZ had a strong imprint on the map-scale fault pattern observable in the Mesozoic and Tertiary sequences. Kinematic analysis of outcrop-scale fracture systems in the latter units yields evidence for local multi-directional extension and strike-slip faulting during Miocene to recent times. While these observations may evoke the interpretation of a multistage palaeostress history along the FBBFZ, slip vector modelling of a very well exposed FBBFZ segment suggests that the various strain records can alternatively be explained by one single regional stress tensor and be related to superordinate deep-seated strike-slip deformation.

Keywords Fault reactivation · Fault-slip analysis · Northern Switzerland · Southern Germany · Alpine foreland · Geodynamics

Introduction

The important role of post-Variscan, Late Palaeozoic basement structures on the Mesozoic and Cenozoic tectonic evolution of Europe has long been recognised (Laubscher 1970; Illies 1972; Ziegler 1992). Some major elements of the European rift system, such as the Rhine and Bresse grabens as well as the connecting Rhine–Bresse transfer zone appear to have formed along preexisting Late Palaeozoic crustal discontinuities (Lacombe et al. 1993; Schumacher 2002; Madritsch et al. 2009). Similar structural interferences between Palaeozoic and Cenozoic structures are also inferred in the immediate foreland of the Alps, for instance the Swiss Molasse Basin (Diebold and Noack 1997; Pfiffner et al. 1997; Malz et al. 2016; Heuberger et al. 2016). While the important role of tectonic inheritance is widely accepted, the detailed structural relationships between inherited Late Palaeozoic precursor structures and younger faults as well as the kinematics resulting from reactivation are less well understood. This is largely due to the fact that outcrops exposing the basement to cover transition of reactivated structures hardly ever exist. This is particularly true for the Swiss Molasse Basin, and information on the structural geological characteristics of this basin

✉ Daniel Egli
daniel.egli@geo.unibe.ch

[1] Earth Sciences Department, Fribourg University, Chemin du Musée 6, 1700 Fribourg, Switzerland

[2] Present Address: Institute of Geological Sciences, University of Bern, Baltzerstrasse 1+3, 3012 Bern, Switzerland

[3] Allmendstrasse 16, 8892 Berschis, Switzerland

[4] Nagra, Hardstrasse 73, 5430 Wettingen, Switzerland

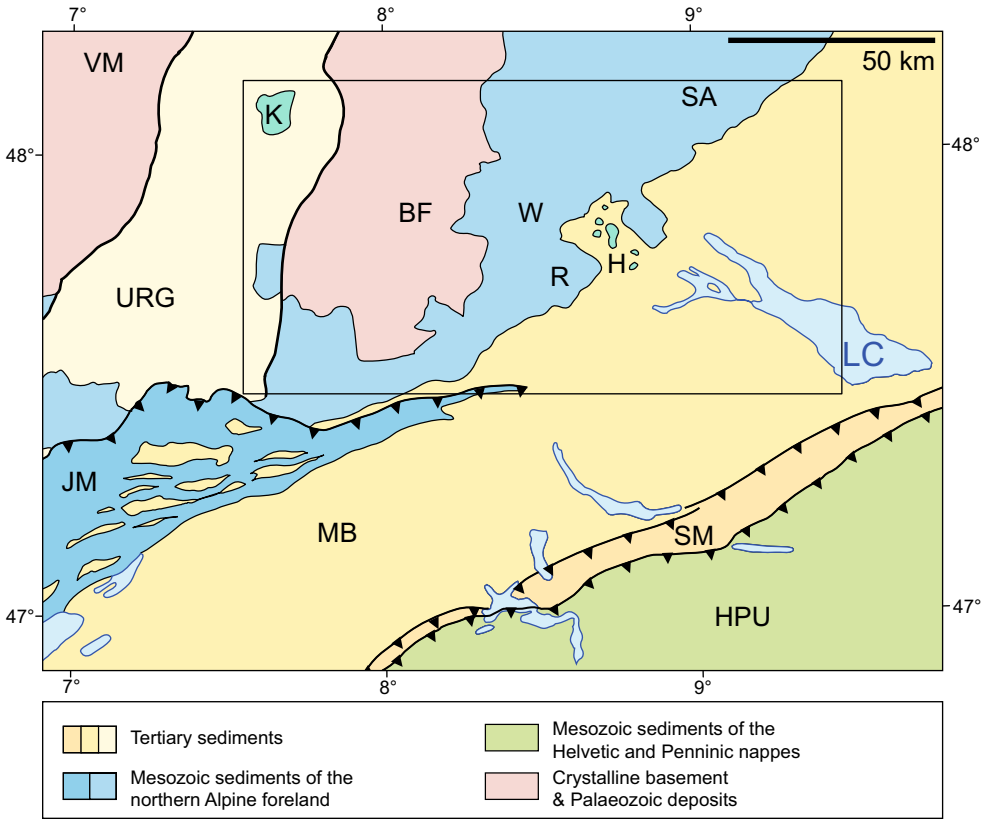

Fig. 1 Overview map of the northern Alpine foreland. The *black box* encompasses the wider study area. *BF* Black Forest Massif, *H* Hegau region, *HPU* Helvetic and Penninic units, *JM* Jura Mountains, *K* Kaiserstuhl, *LC* Lake Constance ("Bodensee"), *MB* Molasse Basin, *R* Randen range, *SA* Swabian Jura ("Schwäbische Alb"), *SM* Subalpine Molasse, *URG* Upper Rhine Graben, *W* Wutach region

is scarce, in particular for those rock units underlying the up to a few-kilometre-thick Tertiary Molasse sediments. Typically, information on rock deformation is available from sparsely distributed drillhole and seismic data (e.g. Sommaruga et al. 2012; Heuberger et al. 2016). Outcrops of Mesozoic and Palaeozoic sediments, as well as the crystalline basement that could provide additional information on structural geological characteristics, are restricted to the edges of the basin. For this reason, the northern rim of the central basin located to the NW of Lake Constance is of particular interest. Due to the shallowly SE dipping strata in this so-called Hegau region, a complete section from pre-Triassic basement rocks of the Black Forest Massif through the Mesozoic cover units into the Molasse sediments and the Quaternary cover can be investigated (Figs. 1, 2).

This study considers the evolution of faults and fault zones along the Freiburg–Bonndorf–Bodensee Fault Zone (FBBFZ), a major WNW–ESE trending deformation zone stretching from the southern Upper Rhine Graben in the NW to the Lake Constance region to the SE (Fig. 2). Its extensive present-day surface trace allows studying the fault zone as it cuts through a wide range of lithologies from the Variscan basement of the Black Forest into the Tertiary sediments of the Molasse Basin west of Lake Constance and as such can serve as a natural analogue for the characterisation of fault structures in the subsurface of the Molasse Basin.

The Miocene to present evolution of FBBFZ and particularly the influence of precursory structures on fault geometries within the cover units are the main focus of this study. The analysis of map- and outcrop-scale structures as well as slip vector modelling is used to develop a kinematic model for the FBBFZ that is discussed in the context of the regions past tectonic and recent geodynamic setting.

Geological evolution and present-day setting

The study area is located in NE Switzerland and SW Germany, reaching from the south-western Black Forest region into the western Lake Constance area (Fig. 1). The study area can be subdivided into four general domains with characteristic morphologic and lithologic features: (1) the hilly landscape of the Black Forest Massif, exposing pre-Mesozoic magmatic and metamorphic sequences (BF in Fig. 1), (2) the Wutach region where fluvial valleys have

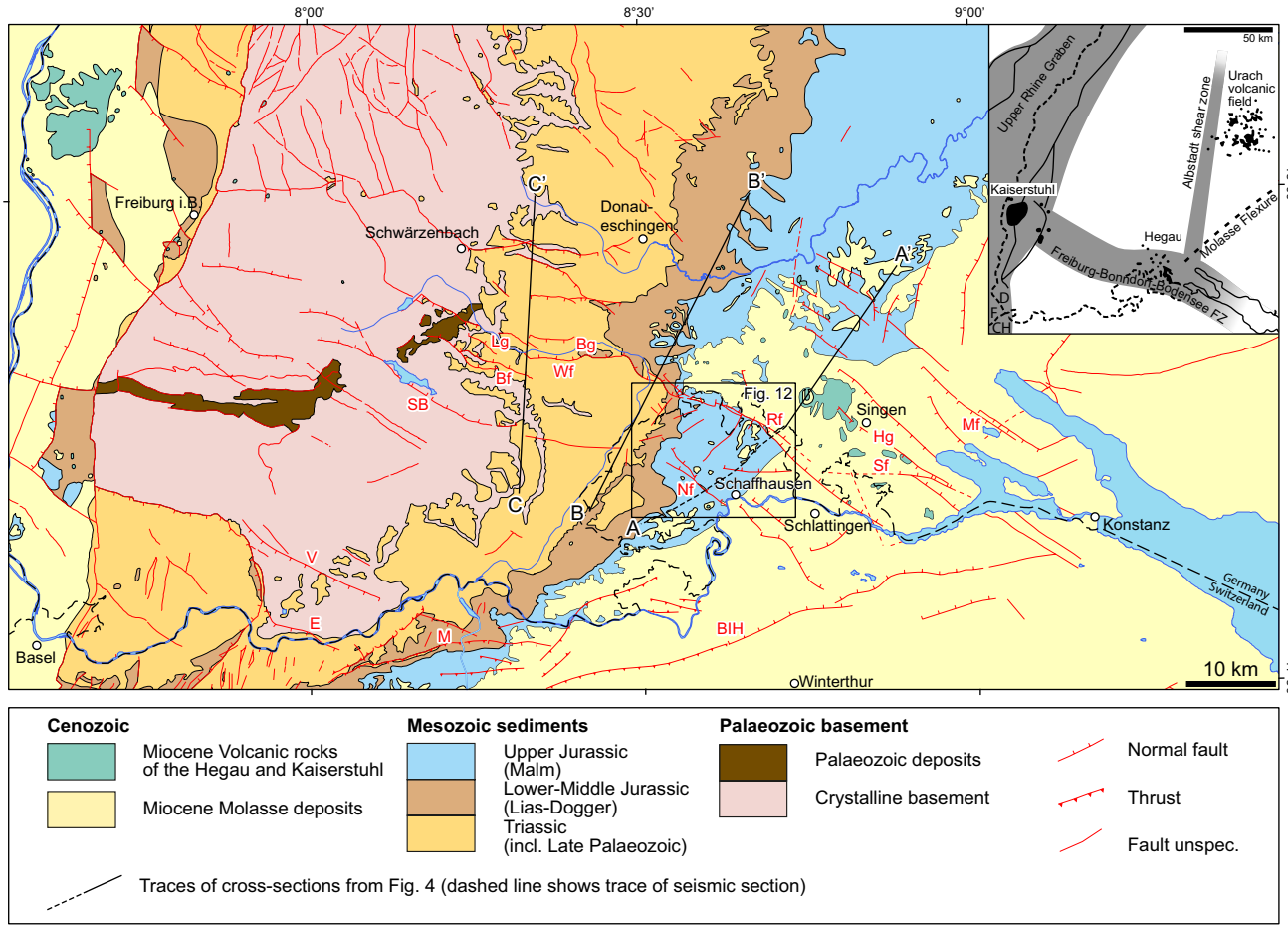

Fig. 2 Geologic map of the larger study area compiled from the Geologic Map of Switzerland 1:500,000 (Swisstopo) and the Geologische Übersichtskarte von Baden-Württemberg 1:300,000 (LGRB). The illustrated faults are taken from the Tectonic Map of Switzerland 1:500,000 (Swisstopo), the Geologische Übersichtskarte von Baden-Württemberg 1:300,000 (LGRB) and NAGRA (2008). Inlay shows the large-scale deformation zones of SW Germany and location of the Kaiserstuhl, Hegau and Urach volcanic fields (redrawn and modified after Geyer et al. 2011). *SB* Schluchsee–Birkendorf faults, *Bf* Bonndorf Fault, *Lg* Lenzkirch Graben, *Wf* Wutach Fault, *Bg* Bonndorf Graben, *Nf* Neuhausen Fault, *Rf* Randen Fault, *Hg* Hegau Graben, *Mf* Mindelsee Fault, *Sf* Schienerberg Fault, *V* Vorwald Fault, *E* Eggberg Fault, *M* Mandach thrust

deeply incised into Middle-Lower Jurassic, Triassic and locally basement rocks (W in Fig. 1), (3) the topographically higher Randen range which is made of Middle-Upper Jurassic limestone and represents the transition between the Tabular Jura of Northern Switzerland and the "Schwäbische Alb" of SW Germany (R in Fig. 1) and (4) the Hegau–Lake Constance region, which is part of the present-day Molasse Basin characterised by flat topography and isolated hills formed by the remnants of the Miocene Hegau volcanoes (H in Fig. 1).

The Black Forest Massif has a heterogeneous composition with widespread occurrence of amphibolite facies ortho- and paragneisses and Carboniferous granitic plutons, as well as tectonised Upper Devonian to Lower Carboniferous metasediments (e.g. Güldenpfennig and Loeschke 1991; Schaltegger 2000; Sawatzki and Hann 2003; Geyer et al. 2011). The basement is overlain by the variably thin Lower Triassic Buntsandstein, followed by Muschelkalk and Keuper series forming the typical succession of the Germanic Triassic. In the study area, the Triassic succession reaches a total thickness of ~250–300 m (e.g. Rupf and Nitsch 2008). It is overlain by Lower (Liassic) and Middle (Dogger) Jurassic series, both characterised by interbedded successions of marls, clay and sandstone. The Upper Jurassic (Malm) series is composed of thick sequences of well-bedded and massive limestones intercalated by marls. An important hiatus exists between the Upper Jurassic and the Eocene due to emersion and erosion during that time.

Pre-Molasse series sediments directly overlying the Upper Jurassic limestones are present as up to 20-m-thick 'Bolustone' of Eocene (and possibly Upper Cretaceous) age as well as Lower Oligocene 'Krustenkalke' (Hofmann

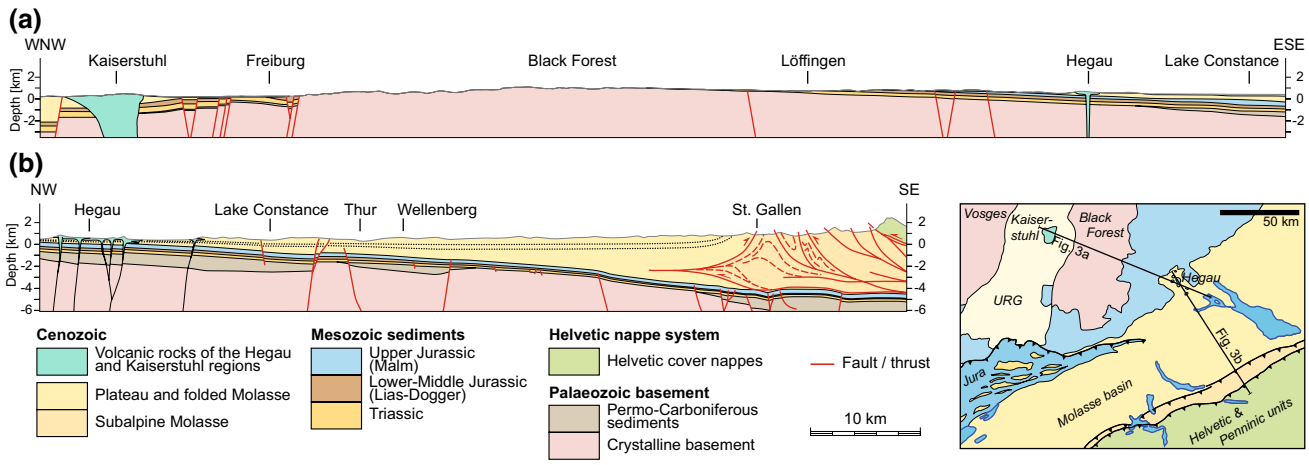

Fig. 3 Cross sections through the larger study region illustrating the overall SE dip of the crystalline basement and the overlying Mesozoic to Tertiary sediments. Cross section **a** redrawn and modified from Rupf and Nitsch (2008), cross section **b** redrawn and modified from Sommaruga et al. (2012)

et al. 2000). Molasse sedimentation in the northern Alpine foreland reached the Hegau region in Chattian times with the deposition of the Lower Freshwater Molasse (USM), followed by the Burdigalian Upper Marine Molasse (OMM) and the ~Langhian to Tortonian Upper Freshwater Molasse (OSM) (Schreiner 1992). The youngest preserved Molasse deposits are reported by Rahn and Selbekk (2007) and accordingly have an age of approximately 10 Ma.

The Cenozoic deformation in the study area is characterised by the interaction between the evolution of the European Cenozoic rift system and the development of the northern Alpine Foreland Basin and in a broad sense the convergence of the Eurasian and Adriatic plates (e.g. Reicherter et al. 2008). Roughly E–W directed rifting of the Upper Rhine Graben, located immediately to the west of the study area (Fig. 1), initiated in Eocene times and developed mainly during the Oligocene, which led to a subsidence of up to several kilometres within that graben (Schumacher 2002; Cloetingh et al. 2006; Hinsken et al. 2007). At least during its Later Miocene evolution, it is associated with transtension with significant sinistral deformation in a NW–SE oriented compressional stress field (Schumacher 2002; Lopes Cardozo and Behrmann 2006; Ziegler and Dèzes 2007). Uplift of the graben shoulders resulted in exhumation of the Black Forest and Vosges Massifs. Flank uplift was further enhanced since Early Miocene by the effect of the north-westward migrating flexural bulge of the northern Alpine foreland (Bourgeois et al. 2007; Ziegler and Dèzes 2007). Previous authors suggested that the extensional Miocene deformation along inherited Palaeozoic structures recognised in the study area was related to this uplift process (e.g. Müller et al. 2002).

The progressive flexural loading of the crust due to the development of the Alps and the uplift of the Black Forest Massif led to a southward dip of the top basement. This is expressed by a wedge-like thickening of the sedimentary succession from the edge of the basin in the NW to a thickness of 1600 m in the Constance area und up to 3000–4000 m at the front of the Alps (e.g. Schreiner 1992; Fig. 3). To the SE of the Black Forest Massif, the base of the Cenozoic and Mesozoic sedimentary stack witnesses a change in regional dip along a lineament striking roughly parallel to the front of the Alps often referred to as "Molasse Flexur" (inlay Fig. 2). In the area N of the FBBFZ, the regional dip is approximately 2° to the SE; south of it the regional dip measures approximately 4°–5°. This indicates a southward increasing influence of the subsidence of the basin due to the loading of the Alpine orogen (Geyer et al. 2011).

Like other areas in SW Germany (Kaiserstuhl, Urach) and Central Europe, the Hegau region was subject to volcanic activity during the Miocene (e.g. Wimmenauer 1974). Absolute age dating, as well as the stratigraphic position of tuff layers within the OSM, indicates that volcanic activity in the Hegau is of Middle to Upper Miocene age (Lippolt et al. 1963; Weiskirchner 1972; Schreiner 1992). The Hegau volcanic field was interpreted to have formed at the intersection of two crustal structures (see inlay in Fig. 2), the N–S trending Albstadt shear zone (Schneider 1979; Reinecker and Schneider 2002) and the WNW–ESE trending Freiburg–Bonndorf–Bodensee Fault Zone (FBBFZ) (e.g. Schmidle 1911; Paul 1948; Carlé 1955).

Erosion since the Latest Miocene to Late Pleistocene removed large amounts of the Molasse deposits and volcanogenic sediments, sculpting the characteristic Hegau morphology with several isolated phonolitic and basaltic conduits forming distinctive cones culminating over the Hegau plane. The estimates concerning the actual extent of Latest Miocene to present Molasse sediment erosion in this part

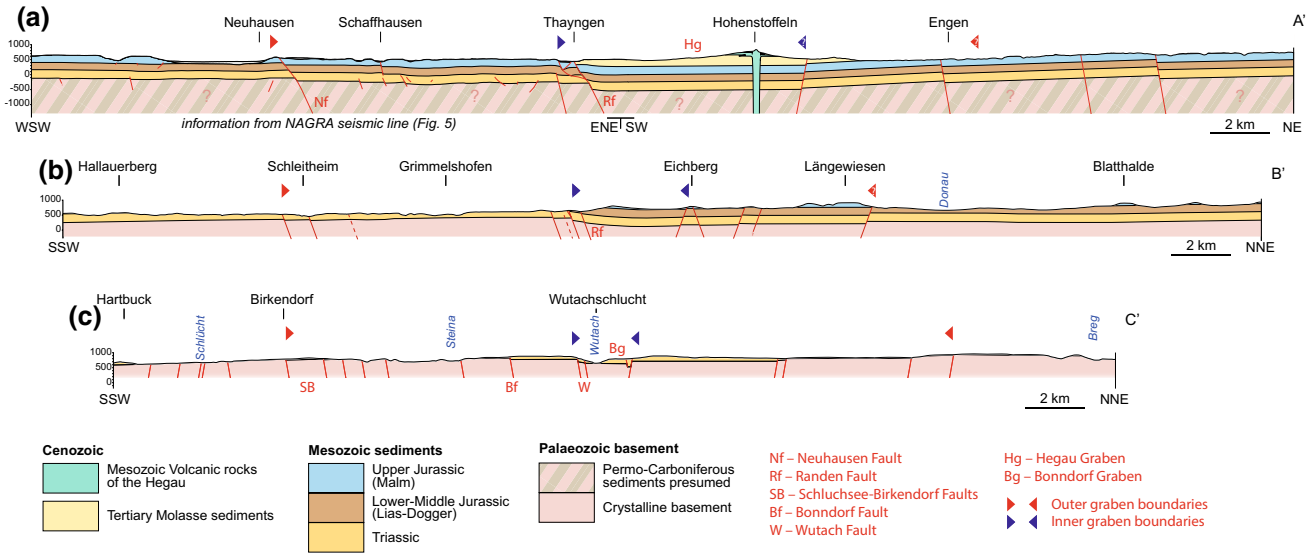

Fig. 4 Cross sections through the FBBFZ illustrating its width and estimated vertical offsets. The inner and outer graben boundaries are rather well defined on the southern boundaries, whereas the northern boundaries are approximate positions. Sections were constructed using 1:25,000 maps of Baden-Württemberg (LGRB) and Switzerland (Swisstopo); the western part of section A–A′ was interpreted from the seismic line 91-NO-79 (Meier et al. 2014). Where no mapped surface or thickness information was available, equal thickness was assumed. Steepness of the faults was estimated from the maps and from the literature

of the NAFB based on thermochronological data differ and range between 1 and 4 km (compare Mazurek et al. 2006; Willett and Schlunegger 2010).

The FBBFZ is the dominating structural feature of the study area and the main subject of this study. It includes a series of NW–SE, WNW–ESE and E–W striking faults and fault systems. From NW to SE, the most prominent fault segments are the Lenzkirch and Bonndorf grabens, the Randen Fault and the Hegau Graben faults (Fig. 2). Fault traces of the FBBFZ are clearly defined by mapped offsets of bedding and morphologic observation at the NW–SE striking Lenzkirch Graben, the southern border of the E–W striking Bonndorf Graben, as well as at the Randen Fault (see also Section "Results"). West of the Lenzkirch Graben, its exact path cannot be traced across the Black Forest basement rocks due to a lack of clear stratigraphic markers. However, several deformation zones, which crudely align, can be followed into the region of the Kaiserstuhl volcanic field in the Upper Rhine Graben (Fig. 2). The two volcanic fields of the Hegau and Kaiserstuhl are thus possibly linked by the FBBFZ (Schmidle 1918; Regelmann and Regelmann 1921; Paul 1948; Geyer et al. 2011). The Randen Fault segment of the FBBFZ represents the northern border of the Randen range, separating Upper Jurassic limestones to the SW of the fault from Molasse sediments that fill the SW part of the Hegau Graben to the NE. Its western part is composed of a complicated network of mainly NE–SW and NW–SE but also differently oriented faults (see Fig. 12). SW of Bibern, the Randen Fault splits into two main splays with a southern NNW–SSE and a northern NW–SE striking branch. The bigger part of the combined NE-down vertical offset of 225 m (Schreiner 1992; Hofmann et al. 2000) is accommodated by the eastern splay, whereas the western splay accommodates approximately 75 m (Fig. 4, A–A′). The exact eastern continuation of the Randen Fault segment into the Molasse Basin remains speculative due to the limited exposure. However, this prolongation is suspected to curve towards the SE. Together with the Schienerberg Fault, it forms the relatively sharp southern border of the Hegau Graben. The northern border of the Hegau Graben is formed by a series of NW–SE striking faults of SW-down kinematics known from correlation of seismic and borehole data (e.g. the Mindelsee Fault; Schreiner 1989, 1992).

Vertical displacement in the central parts of the Hegau and Bonndorf grabens is in the order of 200–250 m during Neogene normal faulting (e.g. Carlé 1955; Schreiner 1989, 1992; Bangert 1991; Hofmann et al. 2000). The fact that no substantial thickness changes of the Mesozoic units occur across the faults indicates a post-Mesozoic main activity. This is corroborated by the correlation of Upper Marine Molasse sediments across the Randen Fault, indicating that the main normal faulting activity took place after the deposition of the Burdigalian "Kirchberger Schichten" and lasted at least until the Late Miocene (Schreiner 1992, 1995; Hofmann et al. 2000). However, there is no clear evidence for the cessation of faulting along the FBBFZ. Outcrop-scale structural observation, low-temperature geochronology, as well as levelling data indicate mid-Miocene to possibly recent

movements along structures between the clearly defined Lenzkirch Graben and the area of Freiburg i.Br. (Freudenberg 1940; Demoulin et al. 1998; Link 2010). Recent seismicity suggests continued activity on related fault segments with a right-lateral and normal fault movement component as indicated by fault plane solutions (Pavoni 1977; Deichmann et al. 2000; Werner and Franzke 2001; Stange and Strehlau 2002; Sawatzki and Hann 2003). Considering these observations, a better understanding of the fault zone's structural and kinematic evolution is desirable.

Investigation approach and methodology

The variable exposure conditions in the study area require a multi-disciplinary approach to decipher its tectonic history and kinematic evolution. During this investigation, a regional compilation of mapped faults for geometric analyses and construction of cross sections is complemented by kinematic analyses of outcrop-scale brittle structures and a slip vector analysis of a particularly well-exposed regional fault structure.

In a first step, published maps were used to establish the extent and the geometry of structures that can be attributed to the FBBFZ in a larger context. Map-scale structures were assessed by comparing fault trace maps digitised from 17 sheets of the geological map of Baden-Württemberg 1:25′000 (Landesamt für Geologie, Rohstoffe und Bergbau [LGRB]) covering the eastern part of the FBBFZ reaching from the Black Forest basement rocks into the Molasse Basin. The evaluated faults were compiled in a synoptic fault trace map and then analysed in terms of their strike, as well as involved lithologies in order to assess changes in fault orientation on a regional scale and particularly across the stratigraphic levels. The results were compared with structural data on smaller-scale structures mapped in the field.

Three N–S to NE-SW geologic cross sections were constructed across the FBBFZ on the basis of surface data, published maps (LGRB and Swiss Federal Office of Topography [Swisstopo]) and the geologic model of Baden-Württemberg (Rupf and Nitsch 2008; Fig. 4). For the western part of section A–A′, a depth-migrated 2D-seismic line was provided by NAGRA. For the construction of the cross section, the published interpretation of the seismic line (Meier et al. 2014, line 91-NO-79) was reinterpreted (Fig. 5).

Geological field investigation, in particular the collection of kinematic data from selected outcrops in the Black

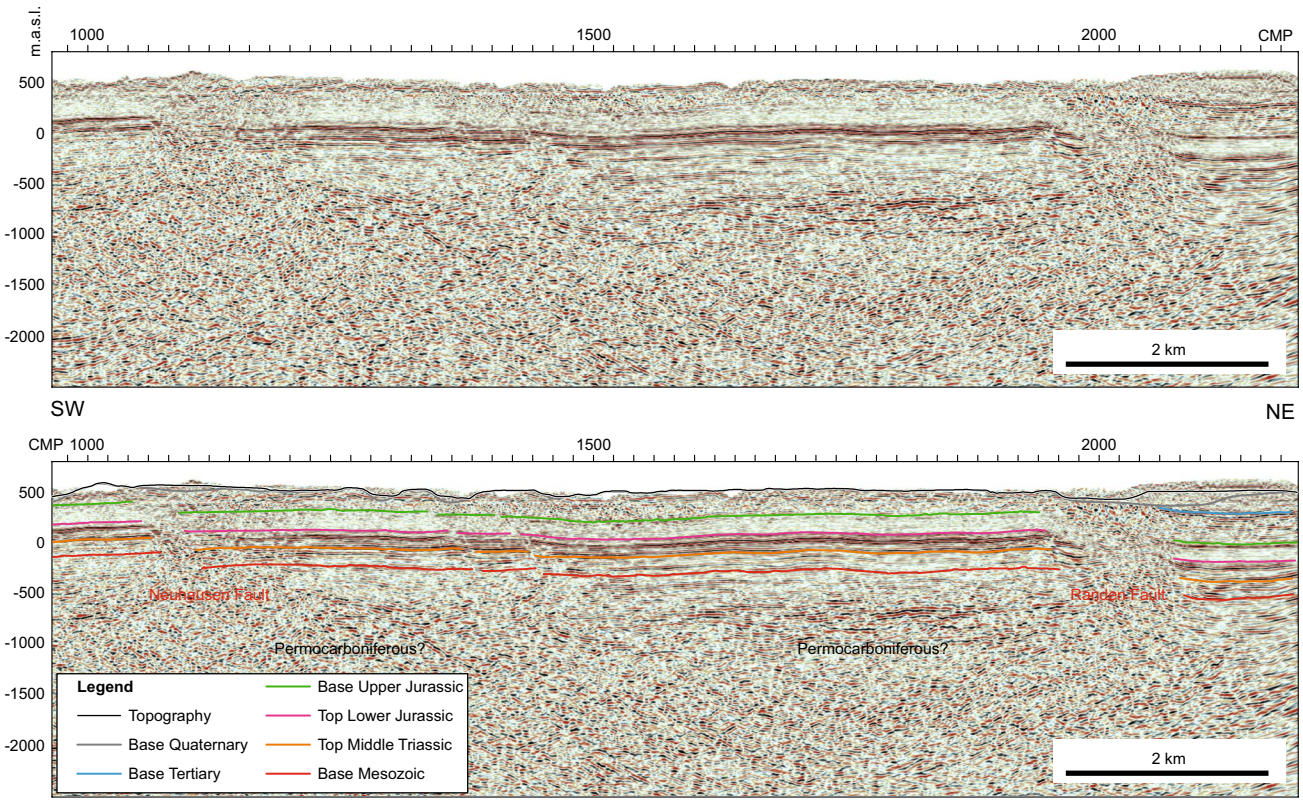

Fig. 5 Excerpt of the NAGRA seismic line 91-NO-79 showing a clear offset of the base of the Mesozoic sediments across the Neuhausen and Randen faults. No thickness changes of the Mesozoic sedimentary units can be observed. Modified after Meier et al. (2014)

Forest–Hegau region, set the basis for this study. However, the poor outcrop situation and frequent absence of striated faults and discernible offset hinder a detailed and extensive palaeostress study on a regional scale. Detailed structural analysis was therefore limited to selected exposures in the Upper Jurassic limestones SW of the Randen Fault, defined as the Randen range in this study, with the main focus on the abandoned quarry of Biberegg near the village Thayngen. The fault-slip data have been sorted manually and processed using the TectonicsFP software (Reiter and Acs 1996–2011; Ortner et al. 2002). Palaeostress reconstruction of the fault-slip data has been performed using the right dihedra method (Angelier and Mechler 1977; Angelier 1994) and the PBT method (Marrett and Allmendinger 1990). The PBT method reconstructs the kinematic axes for every included fault plane and calculates a best fit for the kinematic axes, which can be considered an approximation to the principle stress axes σ1, σ2 and σ3. The right dihedra method is a dynamic approach, restricting the possible orientations of σ1, σ2 and σ3 by overlapping the compressional and tensile dihedra for all included faults, yielding a best fit for the principle stress axes.

In addition to classic fault-slip analysis, we applied slip vector analysis on the Biberegg segment of the Randen Fault. The excellent exposure of the fault's western main splay in this outcrop allowed to extract a 3D fault model from a digital elevation model with a horizontal resolution of 2 m (Source: Swisstopo). Slip vector and stress analysis were conducted using the 3D Stress software [Southwest Research Institute (SwRI)] for theoretical determination of the variations in slip direction and tendency on the complex three-dimensional geometry of the fault plane (see detailed discussion in Section "Slip vector analysis").

Results

Geometric analysis of mapped fault structures and large-scale structure of the FBBFZ

The majority of mapped faults in the Black Forest–Hegau region follow three general strike domains: NNE–SSW, WSW–ENE and NW–SE (e.g. Carlé 1955). The various segments of the FBBFZ, expressed by the large number of E–W to NW–SE striking faults, are the dominating structural feature throughout the study area (Figs. 2, 6).

The Bonndorf and Wutach faults with vertical offsets of ~50 and ~100 m, respectively, border the central and deepest part of the Bonndorf–Lenzkirch Graben to the south (Sawatzki and Hann 2003; Sawatzki 2005). The northern border is less well defined with a series of S-dipping faults. On a broader scale, we consider the southern boundary of the larger graben system to be the Schluchsee and Birkendorf faults (extending to the SE into the Neuhausen Fault) and the northern boundary running from Donaueschingen towards Schwärzenbach as is suggested by Bangert (1991) and Sawatzki (2005), possibly extending to the SE towards the Mindelsee Fault. Including these faults increases the width of the graben system to approximately 20 km in contrast to ~5 km of the central and deepest subsided part (Figs. 2, 4).

The NW–SE striking Neuhausen Fault with downthrow of the north-eastern block is located ~10 km to the SW of the Randen Fault. The zone between the Neuhausen and Randen faults has in recent times been defined as the Hegau–Bodensee Graben border zone (NAGRA 2008). Interpretation of seismic data across the Randen and Neuhausen faults shows an offset in the base of the Mesozoic sequence, indicating basement involved normal faulting (Fig. 5). A more south-easterly segment of the Neuhausen Fault was analysed in great detail in the course of a 3D seismic survey (Birkhäuser and Roth 2001). The high-resolution subsurfaces imaging of the fault yielded distinct en echelon fault segment arrays indicating at least some degree of strike-slip deformation along the structure.

The Schluchsee and Birkendorf faults further to the NW show approximately 60–70-m cumulated offset and align well with the Neuhausen Fault, which has a maximum vertical offset of 80–100 m (Naef et al. 1995; Müller et al. 2002). Although the fault trace between the Schluchsee and the Neuhausen faults is not clearly defined due to insufficient exposure, a correlation between the two structures is assumed. Therefore, this system of southernmost NE dipping faults in our interpretation constitutes the southern border of the extended FBBFZ.

To the NW, the Schluchsee Fault presumably finds its approximate continuation at the northern border fault of the Feldberg Horst. The northern boundary of the extended FBBFZ is concealed in many places and remains speculative.

Despite variable fault orientations on an intermediate scale, the FBBFZ is characterised as a 20–30-km-wide WNW–ESE trending deformation zone running from the Upper Rhine Graben to the Bodensee region. The horizontal stretch over the entire graben structure as reconstructed from the cross sections is on the order of few tens of metres, whereas the vertical offset adds up to 250 m from the graben border faults to the most strongly subsided part of the graben structure (Fig. 4). Along strike, the width of the graben system does not substantially change.

While the WNW–ESE strike of faults clearly dominates in the surface expression, an important number of faults of WSW–ENE orientation have been detected by seismic subsurface mapping (Müller et al. 2002; Interreg_IIIA 2007). This type of faults is particularly common in the eastern and southern parts of the study area in the subsurface of

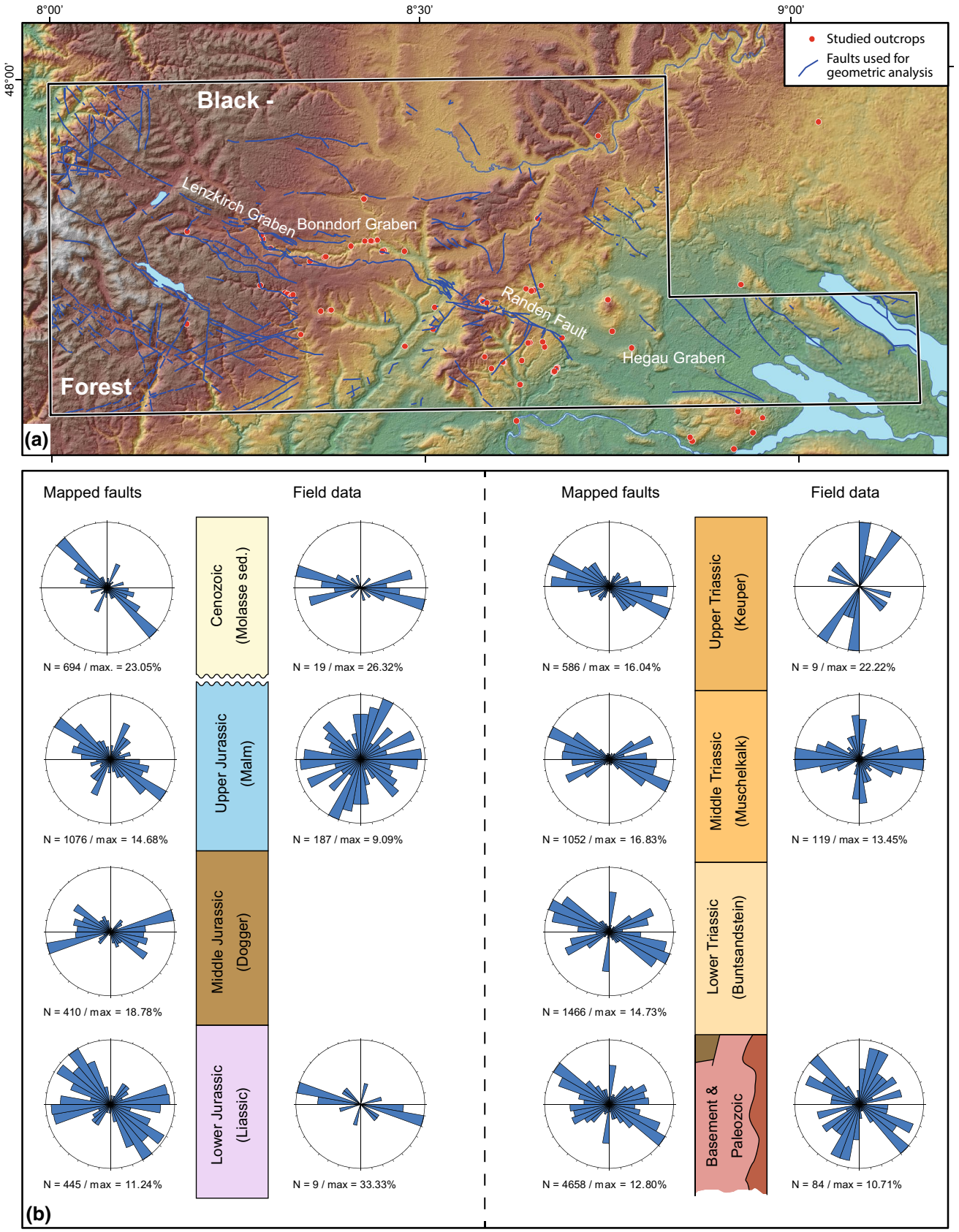
8°00'
8°30'
9°00'
48°00'
Studied outcrops
Faults used for geometric analysis
Black -
Forest
Lenzkirch Graben
Bonndorf Graben
Randen Fault
Hegau Graben
(a)
Mapped faults
Field data
Cenozoic (Molasse sed.)
Upper Jurassic (Malm)
Middle Jurassic (Dogger)
Lower Jurassic (Liassic)
N = 694 / max. = 23.05%
N = 19 / max = 26.32%
N = 1076 / max = 14.68%
N = 187 / max = 9.09%
N = 410 / max = 18.78%
N = 445 / max = 11.24%
N = 9 / max = 33.33%
Upper Triassic (Keuper)
Middle Triassic (Muschelkalk)
Lower Triassic (Buntsandstein)
Basement & Paleozoic
N = 586 / max = 16.04%
N = 9 / max = 22.22%
N = 1052 / max = 16.83%
N = 119 / max = 13.45%
N = 1466 / max = 14.73%
N = 4658 / max = 12.80%
N = 84 / max = 10.71%
(b)

◂**Fig. 6** **a** Digital elevation model, synoptic lineament map used for automated line analysis and location of the studied outcrops (ASTER GDEM is a product of NASA and METI). The faults were compiled from 17 map sheets of the Geological map of Baden-Württemberg 1:25,000 (LGRB). **b** Rose diagrams sorted by lithology for the analysed mapped lineament segments (length weighted) in comparison with measured field data. For explanation see text

the Swiss and German Molasse Basin. The strike of these structures is comparable to the overall orientation of the Molasse Basin, the Molasse Flexure and the Permo-Carboniferous trough of northern Switzerland (Diebold and Noack 1997; NAGRA 2008).

The fault trace map along the eastern part of the FFBFZ compiled on the basis of published geological maps is shown in Fig. 6a and the corresponding strike distribution is depicted in Fig. 6b. Although the general WNW–ESE trend of the FBBFZ is clearly represented throughout all lithologies, there are some marked differences. While in the basement and Lower Triassic units the three main strike orientations are well defined, the Upper Triassic and Lower Jurassic rocks show a less uniform pattern. The poor outcrop situation in the latter units must be considered a source of uncertainty in the distribution of the observed fault directions. As a consequence, the exact trace of the fault zone between the eastern part of the Bonndorf Graben and the Randen Fault remains therefore speculative across the Upper Triassic and Lower Jurassic units (Fig. 2). Furthermore, the E–W striking part of the Bonndorf Graben has a strong influence on the fault strike analysis as it is the dominating feature of this segment of the FBBFZ having a distinct deviation from its general WNW–ESE trend. The dominance of WNW–ESE fault trends and the abundance of NNE–SSW striking faults in the Upper Jurassic Malm units are a result of the nature of the Randen Fault Zone, which is represented by a network of syn- and antithetic faults as well as almost perpendicular to its general trend NNE–SSW striking faults forming a complex cluster of individual faults and tilted blocks (Hofmann et al. 2000). A similar situation of variably striking faults surrounding a major fault plane has been proposed for the subparallel trending Neuhausen Fault (Müller et al. 2002).

Nevertheless, the consistency of the fault orientation across all stratigraphic levels emphasises the importance of inherited fault orientations and precursory structures on the development of the regional faults through geological time.

Field data

General remarks

Outcrop-scale deformation in the study area is mainly reflected by brittle fractures and faults, more rarely accompanied by flexures and local tilting of the strata. Although fracturing is very common, many fractures do not show clear kinematic indicators and/or measurable offset. Good exposure is largely restricted to the basement rocks, the Lower to Middle Triassic sandstone and limestone and the Upper Jurassic Malm limestone. Due to the resulting low spatial density of collectable fracture data useful for kinematic fault-slip analysis, only selected outcrops with a satisfactory number of measurements (>30 faults) are discussed in the following sections. The measurements from the remaining scattered data points were combined and sorted by lithology (Fig. 6b).

The strike of outcrop-scale fractures yields similar preferred orientations as the analysis of mapped faults, although with a larger scatter. In general, the NNE–SSW and WNW–ESE strike prevails in outcrop as well as in map scale. Striated faults often show evidence for both normal faulting and strike-slip movements on single or crosscutting planes. Clear chronologic relationships are often absent, but where such evidence can be found, it tends to show strike-slip deformation overprinting normal faults (Fig. 7a, b). These findings are corroborated by the results of studies on outcrop-scale fracture systems from neighbouring areas to the south (Madritsch 2015) and are in accordance with the general view that a normal faulting phase along the FBBFZ is regionally followed by strike-slip deformation (e.g. Carlé 1955; Geyer et al. 2011). On some fracture planes, curved slickenfibres and striations indicate that the change between normal to strike-slip faulting was progressive (Fig. 7c).

Kinematic field data

The collected outcrop-scale kinematic data have been separated manually for subsequent analyses on the basis of their orientation, their kinematic compatibility as well as crosscutting relationships.

The Biberegg quarry The large Biberegg quarry (47.762°N, 8.683°E) extensively exposes the Randen Fault's western splay (Figs. 8, 12). The outcrop is located on the intermediate block between the two fault branches revealing the western fault surface over a length of approximately 400 m and a height of maximal 50 m (Fig. 8a). The exposed part of the Randen Fault shows a complex geometry with a series of discrete polished undulating surfaces with grooves and corrugations (Hancock and Barka 1987) on the metre and decametre scale (Fig. 8a, b). The smooth tectonically polished planes often enclose up to metre-thick lenses of limestone cataclasites as subslip breccias, in which multiple reworking of cataclasites with fault surfaces is observed (Fig. 8c). The long axes of the lentoid corrugations correlate with the slip direction, which can be determined by calculating a best fit great circle through the poles

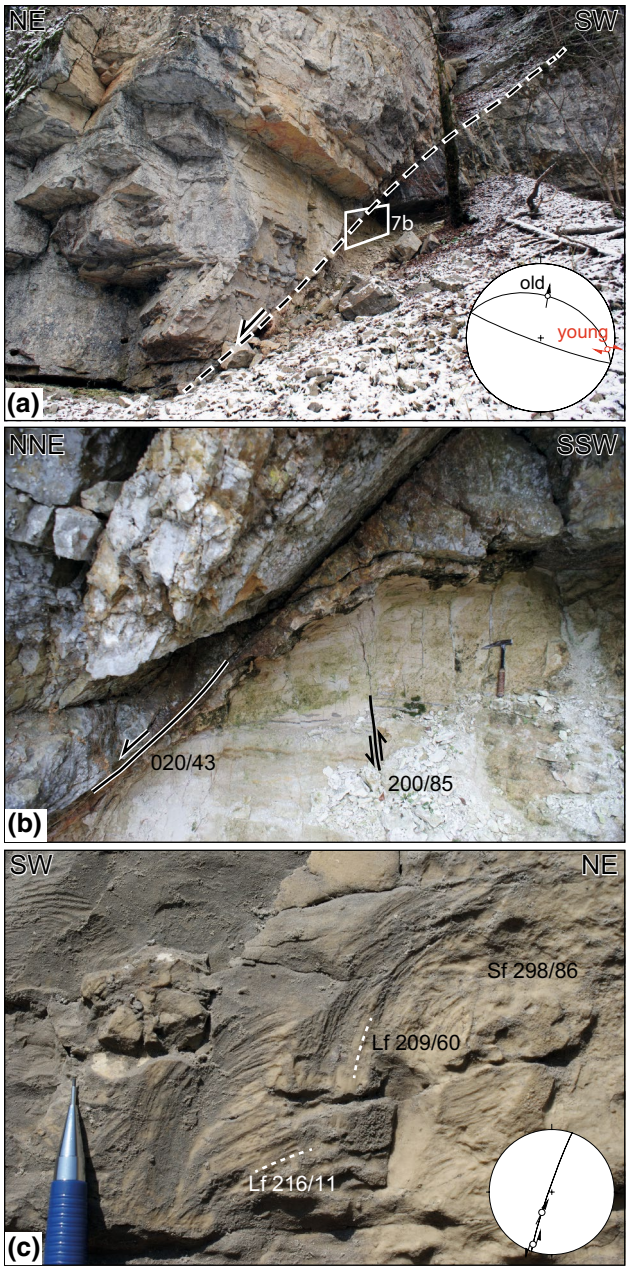

Fig. 7 **a** Example of a fault in the Muschelkalk unit in the Wutach valley (47.84°N, 8.37°E). The main normal fault movement is overprinted by a weak subhorizontal lineation indicating dextral strike-slip movements. The *white box* indicates position of **b**. **b** Close-up of the fault from **a**, showing small conjugate faults to the main fault. **c** Curved striations from the Upper Jurassic Malm *limestone* indicating a progressive change from vertical to strike-slip movements (47.733°N, 8.676°E)

of the curved fault plane, indicating dip-slip movement in an ENE direction (~076/56; Fig. 9). The main fault plane is infrequently crosscut by more steeply dipping to subvertical faults with shallowly plunging striae (Figs. 8d, 10.8). Fault plane measurements at the Biberegg quarry location are dominated by the NW–SE striking main portion of the Randen Fault (Fig. 10.1, 2). The main fault plane is accompanied by smaller antithetic faults with similar strike representing conjugate faults to the main fault (Fig. 10.3). In the fault's hanging wall exposed in the NW part of the quarry, NE–SW trending normal faults roughly perpendicular to the main trend are abundant (Fig. 10.4).

The normal faults exposed in the Biberegg quarry thus show two distinct NW–SE and NE–SW oriented extension directions, although with notable variation (Fig. 10.5). Oblique-slip is very common on the main fault planes, whereas smaller faults tend to show dip-slip lineations. Steep faults with shallowly plunging lineations crosscutting the main fault represent a subsequent event of strike-slip clearly distinguishable by overprinting relationships (Fig. 10.8-1). Strike-slip faults tend to show dextral displacement, but few steep striated faults have an unresolved shear sense. The different populations of subvertical dextral strike-slip fractures show Riedel and P shear geometries relative to the main NW–SE trending fault (Fig. 10.8-2).

Thayngen S and Bargen W locations Fault-slip data in sections in the Upper Jurassic Malm limestone at the locations Thayngen S (47.734°N, 8.678°E) and Bargen W (47.796°N, 8.582°E) (Figs. 11, 12) show normal faulting and subsequent strike-slip movements. At the Thayngen S location, the majority of the striated normal faults strikes NE–SW, which is in strong contrast to the Biberegg quarry further to the east. NW–SE striking faults are also abundant but often do not show a clear lineation (Fig. 11.2). Strike-slip deformation occurs on overprinting steep faults as well as on reactivated normal fault planes (Fig. 11.4). Crosscutting relationships and curved striations indicate that strike-slip movements succeeded the normal faulting. The curved striations imply a progressive change in movement direction. At the Bargen W location situated slightly north of the presumed main trace of the Randen Fault, striated faults can be separated into dominantly NW–SE to E–W striking normal faults and N–S striking (with few exceptions) strike-slip faults (Fig. 11.9–11). The S to SW dipping normal faults apparently form conjugate faults to the main Randen Fault (Fig. 11.10). Strike-slip movements occur on N–S striking vertical faults, showing both sinistral and dextral kinematics. This fault pattern suggests a complex synchronous fracturing into small blocks roughly perpendicular to the S- to SW-down normal faulting direction (Fig. 11.11).

Palaeostress analysis

Dynamic and kinematic fault-slip analysis has been done using the PBT and the right dihedra methods, and both methods overall yield comparable results (Figs. 10.6–7, 10.9–10, 11.5–8, 11.12–13). For the PBT analysis, the best

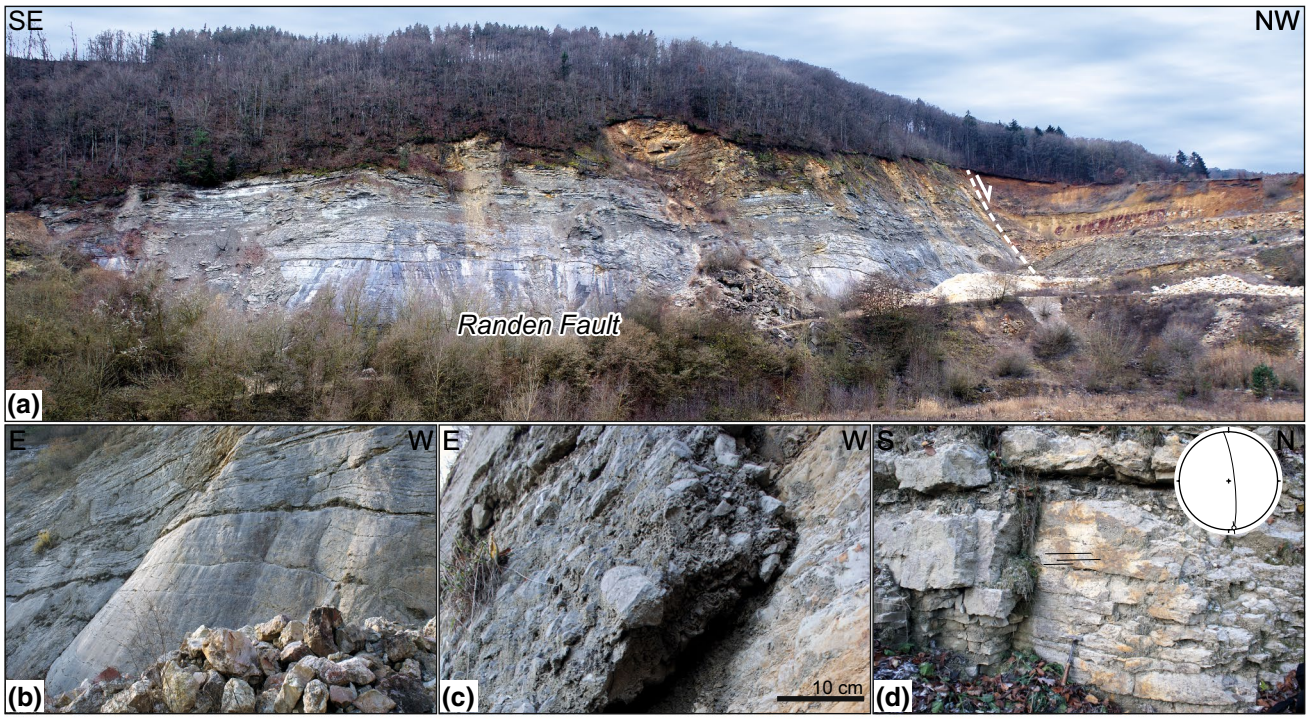

Fig. 8 **a** Panorama view of the Randen Fault plane at the location Biberegg (47.762°N, 8.683°E). **b** Lentoid corrugations of the polished fault surface. **c** Limestone cataclasite in-between the polished parts of the fault planes. **d** Steep crosscutting strike-slip fault

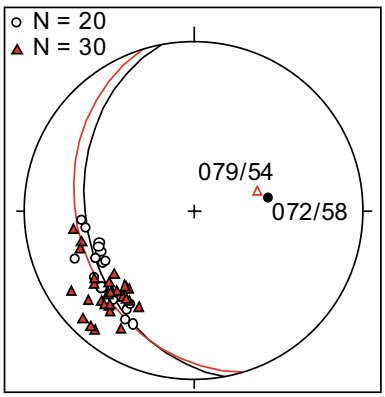

Fig. 9 Lower-hemisphere pole-plots of the Randen Fault plane. *White circles* indicate measurements along two adjacent corrugations; *red triangle* indicates measurements from along the entire outcrop. *Great circles* and their *poles* indicate the respective best fit, and their *poles* represent the hinge of the waves and the presumed movement direction during normal faulting

fit theta angle search function in TectonicsFP was used (for values see Figs. 10, 11), except for the data analysis shown in Fig. 10.9 where a default angle of 30° was used due to an unrealistic best fit calculation.

Given the low density of usable outcrops, the combined kinematic data from the well-exposed Upper Jurassic limestones are taken into account to serve as a proxy for the Cenozoic palaeostress history of the area. According to the overprinting relationships described above, we consider the normal faulting and strike-slip deformation separately in terms of palaeostress reconstruction. For the normal faulting event, two fault sets can be distinguished that could be interpreted in terms of two perpendicular extensions directions (NE–SW and NW–SE; Figs. 10.6, 7, 11.5, 7). No evidence for chronological separation for the extensional events can be observed in the field, and therefore, coeval faulting in both directions must be considered. This pattern of normal faulting in various directions is also represented by the fault trace map of the Randen range between the Neuhausen and Randen faults (Fig. 12) and was also reported by Madritsch (2015) in outcrops north-west of Schaffhausen. The simultaneous occurrence of two perpendicular normal faulting directions could be locally interpreted as a near-radial extension with a constant subvertical σ1 or, alternatively, as a permutation of the σ2 and σ3 directions (cf. Madritsch 2015).

Strike-slip deformation is less abundant than normal faulting and shows a rather scattered distribution (Figs. 10.8, 11.4, 11). The common oblique-slip reactivation of former normal faults and the abundance of Riedel and P shear-type faults result in a large spread in fault orientation. Nevertheless, an approximately regional

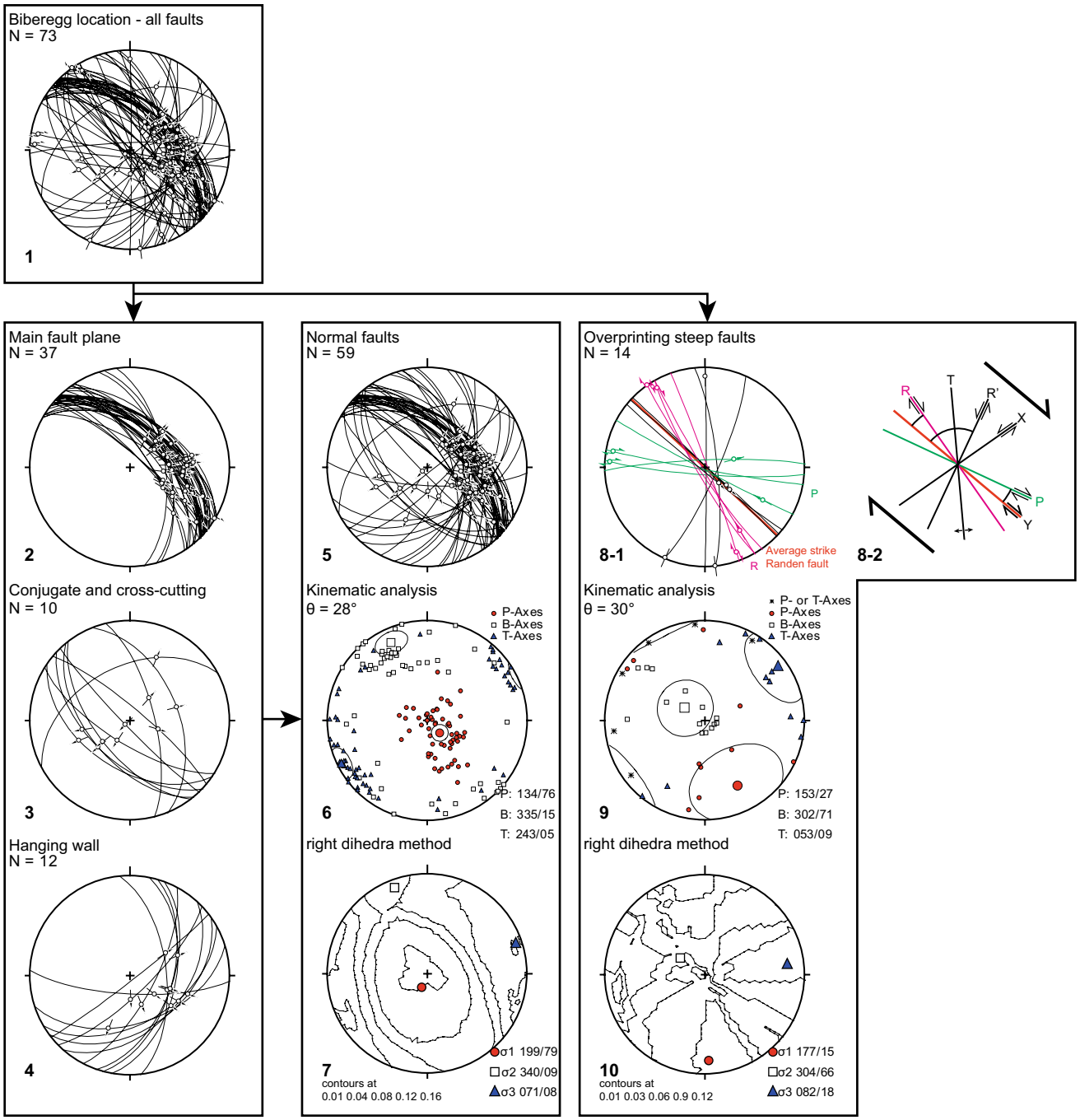

Fig. 10 Lower-hemisphere equal-area plots of the faults at the Biberegg location and PBT and contoured right dihedra plots. Plot 8-1 is a possible interpretation for the different fault orientations taken from theoretical fault orientations in an idealised fault zone with Riedel (R and R′), X, P, and Y shears and the extension fracture T shown in 8-2 (modified after Bartlett et al. 1981)

NNW–SSE to N–S oriented compressive stress field can be derived from both the PBT and the right dihedra analyses, which is comparable to the regional present-day stress field as deduced from earthquake focal mechanisms (Figs. 10.9–10, 11.6, 8; Heidbach et al. 2008; Heidbach and Reinecker 2013).

Slip vector analysis

As described in the previous section, superposition of different movement directions is commonly observed on fault planes exposed in the field. Normal faulting and strike-slip movements are recorded either on one single plane or on

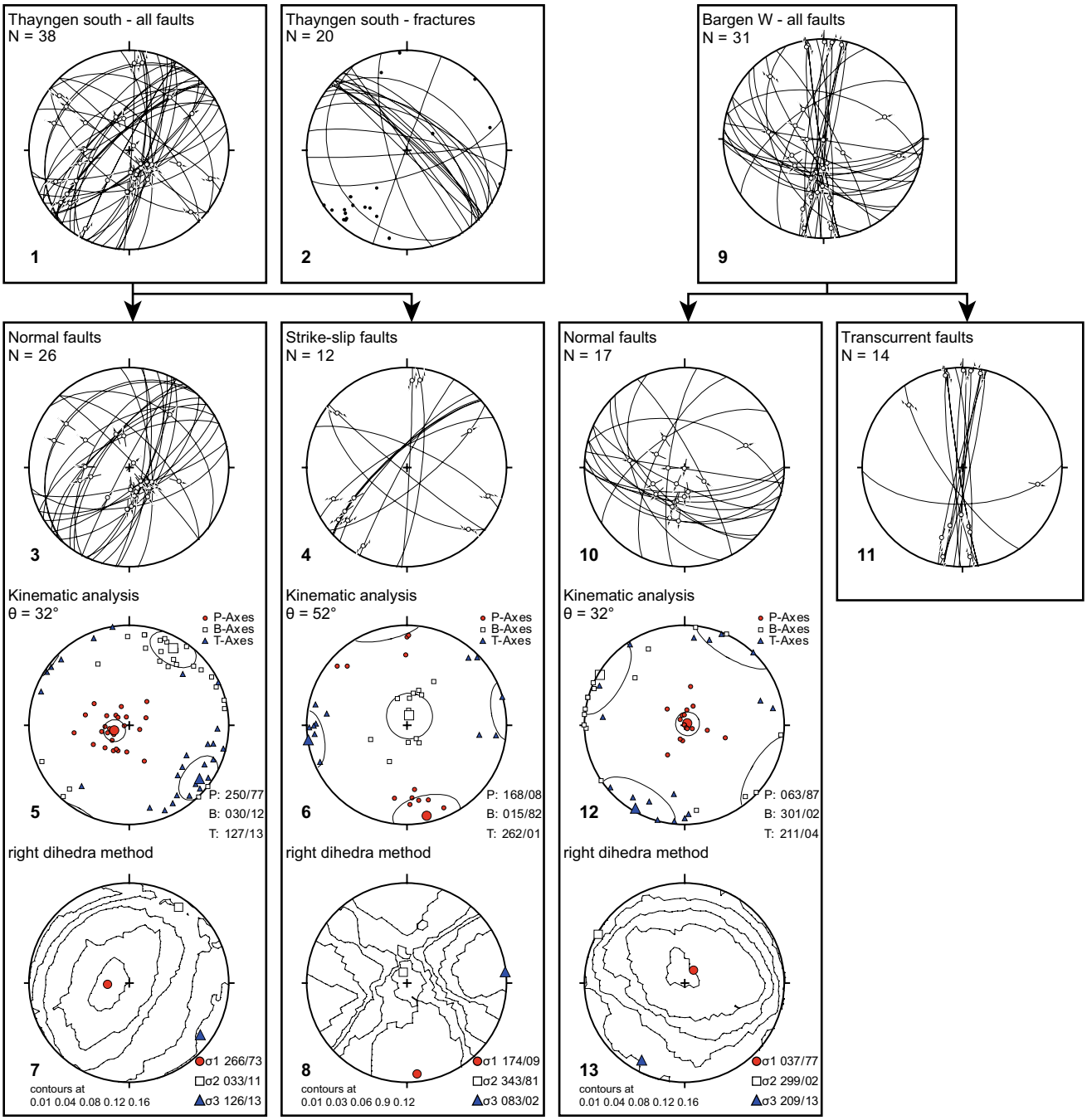

Fig. 11 Lower-hemisphere equal-area plots of the faults at the Thayngen S and Bargen W locations and PBT and contoured right dihedra plots

neighbouring differently oriented faults as well as abundant oblique-slip deformation. Hence, the above-applied separation of fault-slip data yields two different subsequent palaeostress fields with normal and strike-slip faulting kinematics, respectively (see also discussion in Madritsch 2015). However, comparison of the field data and the geometric analysis of mapped fault traces indicate a strong relationship between preexisting fault orientations inherited from basement structures and small-scale deformation along the FBBFZ. Given these indications, the possibility of varying fault-slip kinematics under one single regional stress field as a result of differently oriented precursory structures is explored by means of slip vector modelling. A very well suited case study is provided by the exceptional exposure of the FBBFZ's Randen Fault segment at the Biberegg quarry.

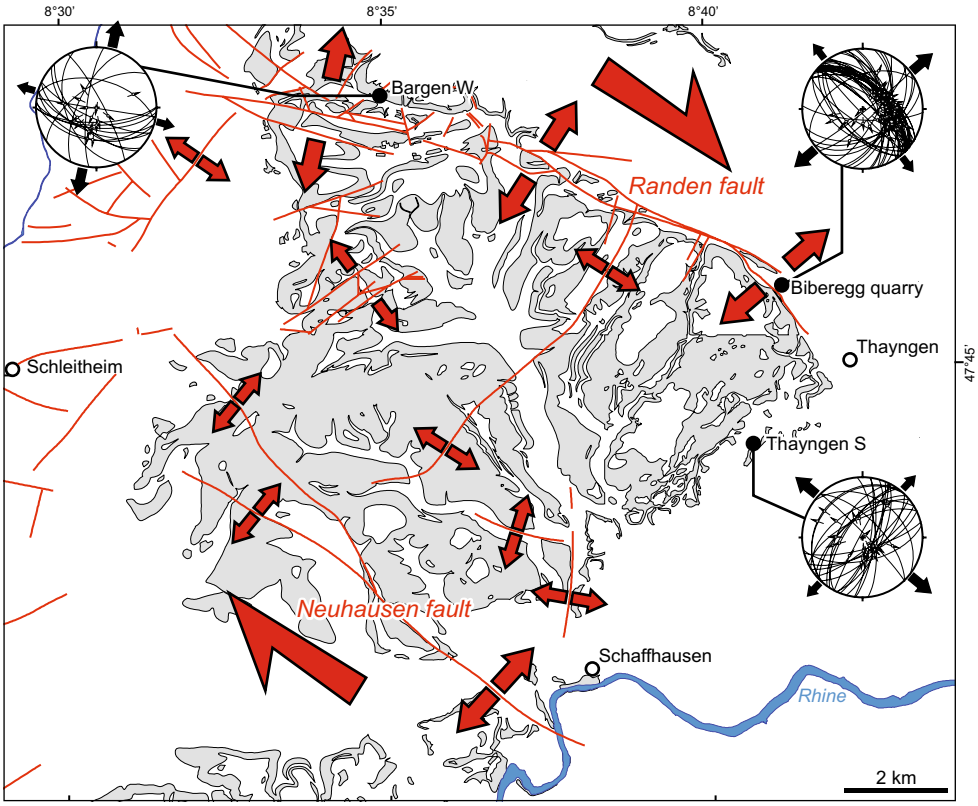

Fig. 12 Kinematic sketch of the Randen range showing extension directions inferred from mapped normal faults (*red arrows*) and from outcrop-scale fault-slip data (*black arrows*, detailed in Figs. 10, 11). The *large red strike-slip arrows* indicate the regionally abundant oblique-slip and strike-slip component commonly observed on the outcrop scale. *Grey shading* outlines the occurrence of Upper Jurassic Malm limestones. Geology and fault traces taken from 1:25,000 geological maps of Switzerland (swisstopo)

Method

In the case of preexisting faults, the slip vector on weakness planes in an ideal case is dependent on the orientation of the plane relative to the stress field and the relative magnitudes of the principal stresses as is stated by the Wallace–Bott hypothesis (Wallace 1951; Bott 1959). The resulting slip direction is therefore parallel to the maximum resolved shear stress on any given plane. The shear stress (τ) and the effective normal stress (σ_n) acting upon a weakness plane are the controlling parameters of slip, where slip is likely to occur, when τ equals or exceeds σ_n and the slip tendency of a surface (T_s) is accordingly defined as the ratio of shear stress to normal stress acting on that surface $T_s = \tau/\sigma_n$ (Morris et al. 1996). The slip tendency analysis method of Morris et al. (1996), which is used in the 3D Stress software (SwRI), utilises this correlation to evaluate slip tendency and, more relevant for this study, provides modelled slip vectors for situations where the orientations and magnitudes of the principal stresses as well as the orientation of structural anisotropies are known.

Parameters and data

The impressive exposure of the Randen Fault at the Biberegg quarry (Fig. 13a) is an excellent opportunity for testing reactivation potential and theoretical slip vectors on a real fault plane and compare modelled values with measured fault-slip data from the field. A 3D fault model with a horizontal spatial resolution of 2 m (Fig. 13b) was extracted from the SwissALTI 3D data set (Swisstopo) and processed using the 3D-Move software (Midland Valley). The full data set consisted of 5970 triangulated surfaces. The large number of surfaces (triangles that were assimilated to fault surfaces in the subsequent analyses) proved too large for comprehensive data presentation, and several levels of subsampling were applied and tested for consistency in the resulting slip tendency and slip vector analysis. The subsampled surfaces yielded comparable results in terms of slip tendency and slip vector. As a consequence, a subsampling of the fault plane to 187 triangulated surfaces was used for further analyses (Fig. 14a–c). As no information on the actual stress tensor is available for this case study, in situ stress estimations derived from hydraulic fracturing tests within a recent geothermal well at Schlattingen, 12 km SE of the Biberegg quarry (see Fig. 2), were used as parameters for the orientation and magnitudes of the principle stress axes (Frieg et al. 2015; Fig. 15a). Four in situ stress tests from depths between 590 and 790 m below surface, of which three stem from the Upper Jurassic limestones and one from the Uppermost Middle Jurassic series, were available. The stress tensors deduced from the hydraulic fracturing tests were used to comparatively evaluate the effect of changing parameters on the predicted slip

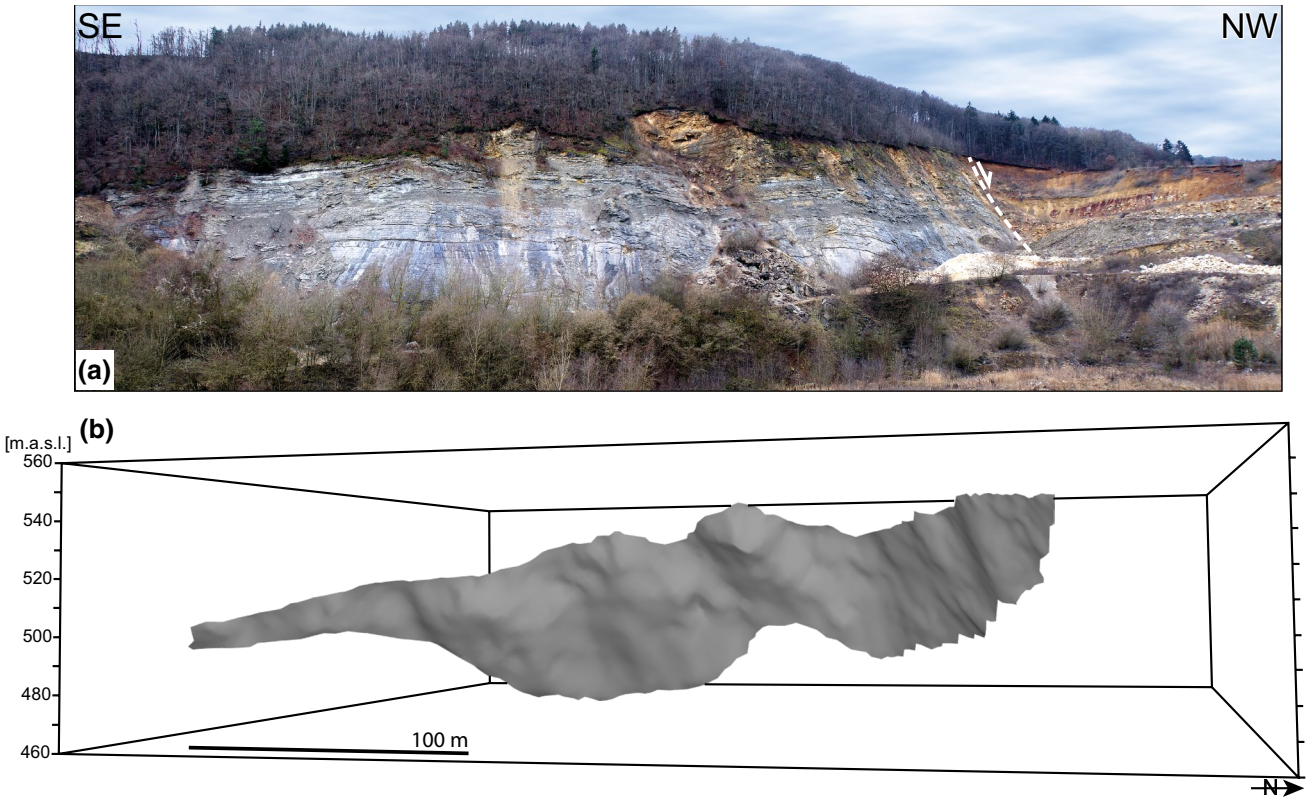

Fig. 13 **a** Panorama of the Randen Fault and **b** the 3D model extracted from the SwissALTI 3D data set (Swisstopo)

vectors and the slip tendency on the Biberegg Randen Fault segment. Assuming an average overburden density of 2.5 g/cm^3, the estimated vertical (Sv), and minimum (Sh) and maximum (SH) horizontal stress magnitudes presented by Frieg et al. (2015) are given in Fig. 15a. These values were used as an approximation to the principle stress axes σ1–σ2–σ3 for our modelling purpose under the assumption that SH is comparable to σ1. The latter is vaguely constrained from earthquake focal mechanisms in the area (Heidbach et al. 2008; Heidbach and Reinecker 2013).

Slip vector analysis results

For each of the in situ stress tests SL1–SL4, the maximum resolved shear stress on all 187 triangles of the virtual fault model were calculated, corresponding to simulated fault-slip pairs consisting of slip plane and slip direction. For the test SL3, we applied two different SH azimuths, the estimated 160° and the average SH azimuth value of 175°. The resulting slip directions on the subsampled Randen Fault model and the 37 fault-slip measurements from the field are shown in Fig. 15b. In all cases, the calculated slip directions are in good agreement with the field measurements from the main Randen Fault plane (Figs. 10.2, 15b). The mean orientation of fault lineations measured in the field is 093/50 and the mean values for the calculated slip vectors are 115/31 (SL1), 117/29 (SL2), 100/49 (SL3, azimuth 160°), 138/03 (SL3, azimuth 175°) and 123/29 (SL4). The results indicate a predominance of oblique-slip movements, which is to be expected during the reactivation of a non-ideally oriented fault. However, the variety of slip directions suggests a possible coexistence of near dip-slip and near strike-slip movements under the same stress field. In the case of the SL3 data, a small change in the azimuth of SH of only 15° from 160° to 175° results in a major difference in the predicted slip directions and a change from dominating strike-slip (for 175°) to an important oblique- and dip-slip movements (for 160°). The relatively small variations of the recent stress estimations thus yield significant changes in the predicted kinematic response along the Randen Fault.

Discussion

The new map- and outcrop-scale structural observations along the Freiburg–Bonndorf–Bodensee Fault Zone provide insights into the Cenozoic tectonic evolution of a major reactivated Palaeozoic precursor structure at the border region between the northern Alpine Foreland Basin and

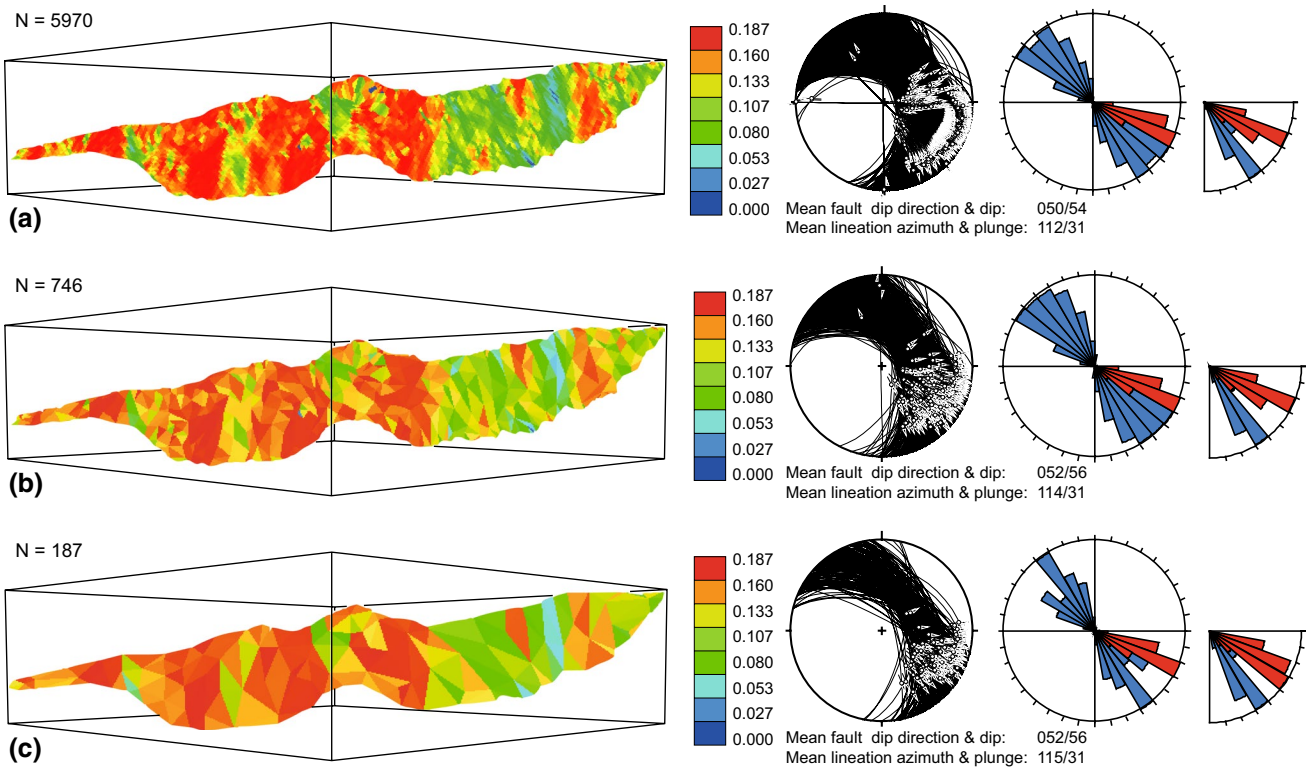

Fig. 14 Comparison of the slip tendency and slip vector analysis using the SL1 stress parameters **a** on the full 3D model, **b** on a model subsampled to 746 triangulated surfaces and **c** subsampled to 187 surfaces. The *rose diagrams* indicate the strike and dip of the planes (*blue*) and the dip direction and plunge of the calculated slip vector (*red*)

the Black Forest Massif. In the following sections, the integrative interpretation of the various study results are discussed in terms of the fault zone's large-scale geometry and its kinematic and geodynamic evolution.

Regional scale and depth interpretation

On the large scale, the FBBFZ represents an on average 20–25-km-wide WNW–ESE trending zone of normal and strike-slip faulting, forming a graben structure with subsidence of up to 250 m in its central part. Its south-western border is well defined by the Neuhausen and Schluchsee–Birkendorf faults. The northern rim of the graben zone is less well defined. Nevertheless, known structures such as the Mindelsee Fault as well as the northernmost boundary of the Bonndorf and Lenzkirch grabens mark its approximate maximum extent to the north (Fig. 2). The most prominent fault segments, the Bonndorf Graben and the Randen Fault, are framed by a more distributed zone of deformation belonging to the same fault system.

Offset of the basement–cover boundary in the Lenzkirch–Bonndorf area indicates direct deformation coupling between the crystalline basement exposed in the middle section of the FBBFZ and the sedimentary cover preserved further to the SE. In the latter area, a seismic section along the western part of section A–A′ (Figs. 4, 5) shows that the eastern segments of the Neuhausen and Randen faults, and probably also many smaller faults, reach into the basement. Therefore, the basement fault geometry must be considered to exert a prime control on Cenozoic deformation in the Randen-Hegau region. The predominance of WNW–ESE to NW–SE striking faults across all scales indicates an inheritance and reactivation of older post-Variscan basement faults as was already proposed by previous authors (e.g. Carlé 1955; Geyer et al. 2011). The extent of the graben zone and its length of nearly 100 km points towards a major crustal-scale deformation zone.

Kinematic considerations

As outlined above, the Mesozoic and Cenozoic regional-scale fault pattern observable along the FBBFZ appears to be strongly controlled by the inheritance of precursor structures. Most probably the latter process also exerted a strong control on the outcrop-scale fault patterns observed within the Mesozoic and Cenozoic units of the Hegau region. It is therefore imperative to consider local stress variations, common in the vicinity of larger faults (e.g. Homberg et al.

(a)

	SH [MPa]	Sv [MPa]	Sh [MPa]	Azimuth (SH)	Depth (below ground)	Mean slip direction ■
SL1	14	**14.5**	10	3°	590 m	115/31
SL2	**17.5**	16.5	11	175°	680 m	117/29
SL3	**23**	18	15.5	160° / 175°	730 m	100/49 - 138/03
SL4	**21**	19	14	180°	790 m	123/29

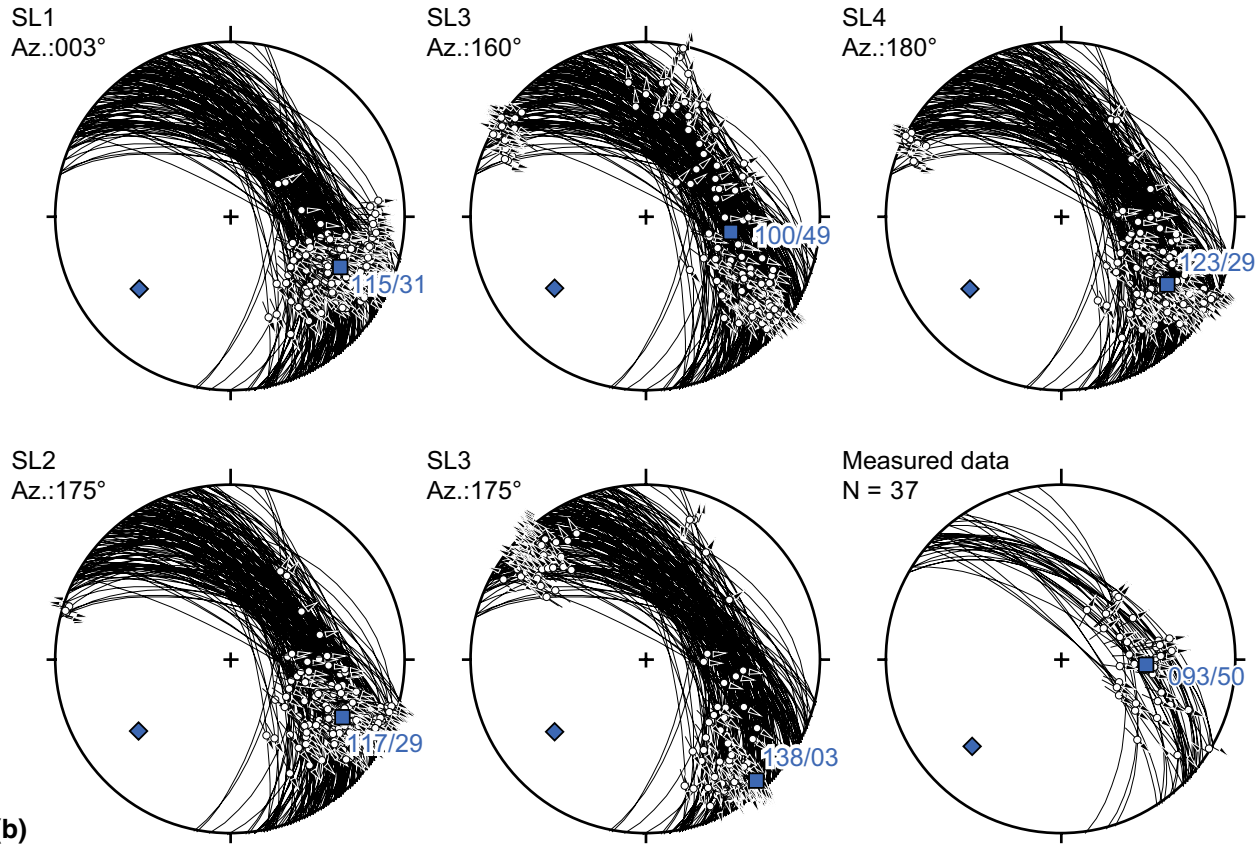

Fig. 15 **a** Parameters used for fault-slip modelling refer to in situ stress data derived from hydraulic fracturing tests within the Schlattingen borehole (Frieg et al. 2015) including estimations for magnitude and azimuth of the stress axes and the measurement depth (from surface). For the shallowest test (SL1), Sv shows the largest stress magnitude whereas for the remaining three tests SH shows the largest value. *SH* maximum horizontal stress, *Sh* minimum horizontal stress, *Sv* vertical stress. **b** Resulting slip vectors under the various stress conditions. Mean orientation of the modelled fault surface is 052/56; mean orientation of the measured fault planes is 046/60. The *blue diamond* indicates the pole of the mean fault plane orientation; the *blue square* indicates the mean slip vector

1997), during the kinematic analysis of the outcrop-scale field data and regional palaeostress field interpretations. According to initial field observations (see Section "Field data"), the study area's Miocene brittle deformation history is characterised by multi-direction normal faulting subsequently followed by strike-slip faulting. Considering the above-mentioned setting and the implications from our slip vector modelling (Section "Slip vector analysis"), the tectonic interpretation of these field observations need to be cautious.

Normal faulting occurred on dominantly NW–SE and less commonly on NE–SW striking faults. Based on stratigraphic constraints, dominant NE–SW directed normal faulting started around Middle Miocene times. The less common NE–SW striking normal faults, orientated perpendicular to the main NE–SW extension direction, are

particularly common in the Randen range (Madritsch 2015; this study). The timing of activity is not well constrained, but crosscutting relationships suggest that these faults formed simultaneously to the NW–SE striking ones. For this reason, polyphase normal faulting with one or multiple permutations of the σ2 and σ3 directions appears unlikely. Alternatively, the multi-directional normal faulting could be interpreted as radial extension (i.e. vertical σ1 and equal σ2 and σ3 magnitudes). As was discussed by Madritsch (2015), such a stress field may result from extensional reactivation of deep-seated structures of varying strike, possibly in relation with the uplift of the Black Forest Massif and its southward adjacent flank (Müller et al. 2002). While this interpretation approach is acceptable, clear evidence for deep-seated structures whose reactivation could effectively lead to directed NE–SW normal faulting (e.g. ENE–WSW striking Permo-Carboniferous basin) are not robustly constrained for the area north of Schaffhausen (Marchant et al. 2005; Ibele 2015). More importantly, the PBT analysis of the fault data sets observed in the field reveals a rather bimodal than radial distribution of T-axes (see Figs. 10.6, 11.5). Therefore, and for other reasons outlined below, we favour a different interpretation to explain the observed outcrop-scale normal fault pattern.

In the field, evidence for oblique-slip during the above-mentioned normal faulting phase indicates a non-negligible component of dextral horizontal movements already before a subsequent phase of strike-slip deformation along the FBBFZ. In the case of the NW–SE striking Neuhausen Fault, en echelon fault arrays imaged by a high-resolution seismic survey (Birkhäuser and Roth 2001) may also suggest a dextral strike-slip component during NE–SW directed normal faulting. Since the less commonly observed NW–SE striking normal faults apparently formed simultaneously to the NE–SW striking ones, these faults might also be explained in the context of strike-slip to transtensional deformation. In the Randen range that is located between the prominent and westward converging Neuhausen and Randen faults, these structures may represent compensational normal faults analogous to a small-scale releasing bend in between these two NW-converging faults (Fig. 12). The same mechanism could be responsible for the NE–SW striking normal faults in the Biberegg quarry (Fig. 10.4). This interpretation allows explaining the multi-directional normal faulting observed at the outcrop-scale by larger-scale strike-slip deformation mechanism. For adjacent areas in the north, it has been discussed by Schwarz (2012) that even though dominant deformation mode is strike-slip, an important amount of vertical motion can occur that does not necessarily have a primary genetic importance.

The case study of the Randen Fault at the Biberegg quarry presented here allows demonstrating the compatibility of the various observed movement directions in a constant stress field by slip vector modelling. The unique possibility to carry out a detailed comparison of palaeostress, recent stress and predicted fault-slip on preexisting planes emphasises the problem of incongruous fault-slip data to derive a coherent solution on the stress field. While kinematic analyses alone might suggest a multi-phase deformation history including several changes in the stress field—at least two in our study area—modelling of slip vectors using preexisting fault planes in combination with information on the current stress field allows an evaluation of the palaeostress calculations. The fact that the application of recent stress values to the 3D model of the Randen Fault results in a slip vector pattern that strongly resembles the measured fault-slip data lead us to suggest that, under the assumption that the geometry of the fault is defined by an inherited structure, the formation of the Randen Fault in Middle Miocene times could have formed under a stress field comparable to the present-day situation. Furthermore, the slip vector analysis demonstrates that small fluctuations of stress azimuth and magnitudes (e.g. due to changing fluid pressure) can have relatively large effects on slip directions forming as a response on preexisting planes.

Overall, we infer that no major changes in the stress field are necessary to form the observed structures. A regional strike-slip regime on a crustal scale with a sub-horizontal largest principle axis of stress comparable to the recent stress field is capable to explain the deformation features observed in the field. Possibly, the same stress field has already been active during the Middle Miocene. The observed normal faulting is also explainable in such a regional tectonic setting and presumably the consequence of local stress variations and/or tectonic inheritance (Fig. 16).

Geodynamic implications

The large-scale structure of the FBBFZ is interpreted as a subvertical crustal-scale fault zone, whose present geometry is largely inherited from post-Variscan or older faults. The overall vertical offsets in the order of 250 m compared to its length of >100 km and width of 20–30 km are relatively small. Our large-scale observations concerning the structure of the FFBFZ (e.g. large lateral extent opposed by comparatively small fault throws) combined with the new fault-slip field data, and conclusions drawn from slip vector modelling lead us to interpret that, at least since the Middle Miocene, large-scale strike-slip tectonics were the dominating mechanism along this fault zone. The deformation resulted in multi-directional but dominantly NE–SW directed normal faulting that is widely observed along its south-eastern segment dissecting the Molasse Basin in the Hegau area. This normal faulting and the related evolution

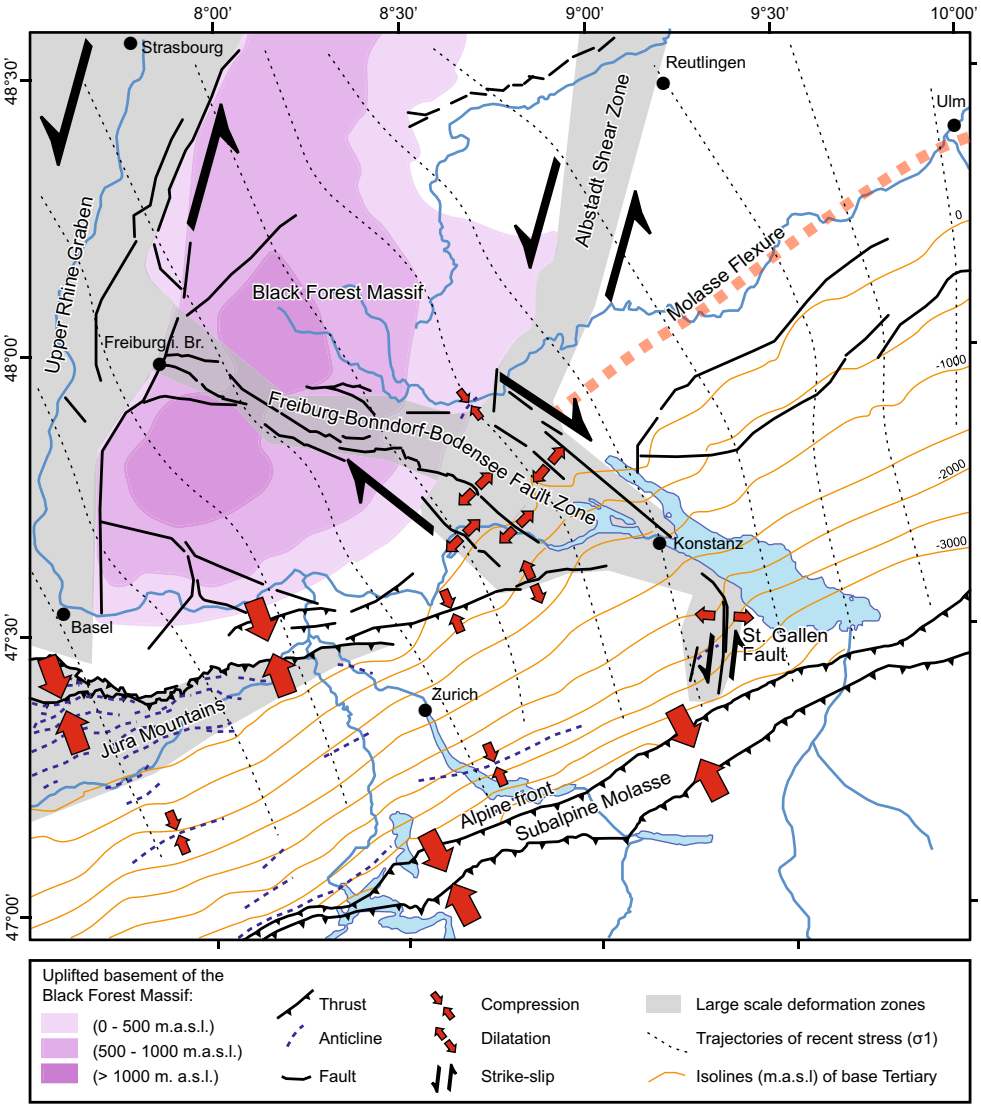

Fig. 16 Large-scale kinematic model showing a selection of important deformation zones and summarising the deformation pattern in the northern Alpine foreland. The interpretation of the Freiburg–Bonndorf–Bodensee Fault Zone as a large-scale conjugate strike-slip structure to the URG, the Albstadt shear zone as well as the St. Gallen fault is compatible with the estimated trajectories of the recent stress field taken from Heidbach et al. (2008)

of graben structures are considered a local kinematic response to that crustal-scale strike-slip. Such an interpretation allows explaining all the observed structures and palaeostress reconstructions without a distinct geodynamically significant phase of NE–SW directed extension. It is also corroborated by the results of a SW-ward adjacent more regional palaeostress study suggesting that normal faulting in the Randen area is a rather local phenomenon and cannot be associated with a regionally recognisable palaeostress field (Madritsch 2015). On a crustal scale, it has been discussed by Stange and Strehlau (2002) on the basis of fault plane solutions that, although strike-slip occurs more frequently in the upper crust than normal faulting, in some cases horizontal or vertical σ1 orientations can fit the data equally well, which is an observation comparable to our surface data on an entirely different scale. Although the question for what causes this ambiguity of σ1 orientation remains (Stange and Strehlau 2002), we hereby propose a possible model for the near-surface portion of the upper crust.

The FBBFZ and the Albstadt shear zone could represent a conjugate fault system. The latter structure has been defined as a zone of enhanced seismic activity running ~N–S from the Hegau region towards the Urach volcanic field (Fig. 16), hosting some of the strongest recent earthquakes in Central Europe (Schneider 1993; Reinecker and Schneider 2002; Stange and Brüstle 2005; Reicherter et al. 2008). This observation, together with the fact that the strike-slip kinematics of FBBFZ proposed here are also well compatible with the present-day stress field (Heidbach and Reinecker 2013), suggests that ongoing tectonic activity along the FBBFZ cannot be entirely excluded. In fact, such activity is vaguely suggested by recent seismicity (Deichmann et al. 2000).

Conclusions

The Freiburg–Bonndorf–Bodensee Fault Zone (FBBFZ) is considered here as a deep-seated, steep NW–SE striking deformation zone, which inherited its architecture from Late Palaeozoic times. The structure acts as a zone of moderate strike-slip movements at least since the Middle Miocene as a consequence of reactivation under the far-field stresses induced by the Alpine compression. Newly collected structural data from the Black Forest–Hegau–Lake Constance region, in combination with geometric analysis of previously published maps, palaeostress analysis and slip vector modelling on nonplanar fault surfaces lead us to draw the following conclusions:

1. The FBBFZ represents an approximately 20-km-wide graben structure with a 5-km large central part exhibiting a maximum normal offset of some 250 m.
2. The orientation trend of Palaeozoic precursory structures can be traced from the basement through all stratigraphic units up into the Neogene sediments of the Molasse Basin. It is therefore likely that post-Palaeozoic deformation within the study area is mainly controlled by reactivation of preexisting structures associated with the FBBFZ.
3. Palaeostress tensors calculated from outcrop-scale faults and fractures yield variable directions of extension constrained by roughly two sets of normal faults and strike-slip deformation. Due to the fact that the transition from normal to strike-slip faulting appears to be gradual in places and the indications given by slip vector modelling that normal and strike-slip increment may potentially be caused by one and the same stress field, we infer that the observable deformation features are indicative for local strain perturbations rather than regional palaeostress states. The local fault pattern is thus not necessarily indicative of the overall geodynamic setting.
4. This interpretation suggests that the comparatively complex outcrop-scale fault kinematics observed in the Black Forest–Hegau region are compatible with a Palaeozoic precursor structure's reaction to the far-field push of the Alpine orogeny and that the related regional stress field was probably relatively constant from Middle Miocene to present times.
5. In the given case study, the formation of locally differing outcrop-scale deformation patterns including the frequently observed normal faulting is interpreted to not be related to a multistage palaeostress evolution but to be caused by the deep-seated reactivation of the preexisting FBBFZ in an overall strike-slip mode. This interpretation allows explaining the region's Miocene to recent deformation history with one, relatively constant stress field tensor.
6. Reactivation of non-ideally oriented faults and fractures strongly influence local deformation patterns along the FBBFZ and hamper reliable geodynamically valid palaeostress reconstructions. Modelling a complex fault surface and comparing the results with measured slip data shows that the variety of slip directions is due to the coexistence of near dip-slip and near strike-slip movements generated by the same stress field. Small changes in stress magnitudes may lead to significant changes in the slip movement directions. Thus, slip vector analysis proves to be a useful alternative/addition to classic fault-slip analysis for understanding incongruous fault-slip data.

Acknowledgements This study was funded by the Swiss National Science Foundation (SNF Projects 200021_144145 and 200020_156252) with kind support of the Swiss National Cooperative for the Disposal of Radioactive Waste (NAGRA). NAGRA's permission to publish parts of the 2D reflection seismic profile 91-NO-79 is particularly acknowledged. We thank K. Reicherter and H. Ortner for critical, yet constructive reviews and W.-Chr. Dullo (Chief Editor, IJES) for the support and manuscript handling.

References

Angelier J (1994) Fault slip analysis and palaeostress reconstruction. In: Hancock PL (ed) Continental deformation. Pergamon Press, Oxford, pp 53–100

Angelier J, Mechler P (1977) Sur une méthode graphique de recherche des constraintes principales également utilisable en tectonique et en séismologie: la méthode des dièdres droits. Bulletin de la Société Géologique de France XIX(7):1309–1318

Bangert V (1991) Blatt 8115 Lenzkirch. Geologische Karte von Baden-Württemberg 1:25 000, Erläuterungen: p 132

Bartlett WL, Friedman M, Logan JM (1981) Experimental folding and faulting of rocks under confining pressure Part IX. Wrench faults in limestone layers. Tectonophysics 79(3):255–277

Birkhäuser P, Roth P, Naef H et al (2001) 3D-Seismik: Räumliche Erkundung der mesozoischen Sedimentschichten im Zürcher Weinland. Nagra Technical Report, NTB 00–03, Wettingen, p 158

Bott MHP (1959) The mechanics of oblique slip faulting. Geol Mag 96(02):109–117

Bourgeois O, Ford M, Diraison M et al (2007) Separation of rifting and lithospheric folding signatures in the NW-Alpine foreland. Int J Earth Sci 96(6):1003–1031

Carlé W (1955) Bau und Entwicklung der südwestdeutschen Grossscholle. Geologisches Jahrbuch, Beihefte 16:272

Cloetingh S, Cornu T, Ziegler PA et al (2006) Neotectonics and intraplate continental topography of the northern Alpine Foreland. Earth Sci Rev 74:127–196

Deichmann N, Ballarin Dolfin D, Kastrup U (2000) Seismizitat der Nord- und Zentralschweiz. NAGRA NTB00–05, p 93

Demoulin A, Launoy T, Zippelt K (1998) Recent crustal movements in the southern Black Forest (western Germany). Geol Rundsch 87(1):43–52

Diebold P, Noack T (1997) Late Palaeozoic troughs and Tertiary structures in the eastern folded Jura. In: Pfiffner OA, Lehner P, Heitzmann P et al (eds) Deep Structure of the Swiss Alps: results of NRP 20. Birkhäuser, Basel, Switzerland, pp 59–63

Freudenberg H (1940) Eine Kartierung der Bewegungsspuren im obersten Höllental (Schwarzwald). Geol Rundsch 31(3–4):285–293
Frieg B, Grob H, Hertrich M et al (2015) Novel approach for the exploration of the Muschelkalk Aquifer in Switzerland for the CO2-free production of vegetables. In: Conference Abstract: Proceedings World Geothermal Congress 2015, Melbourne, Australia, 19–25 April 2015
Geyer M, Nitsch E, Simon T (2011) Geologie von Baden-Württemberg. Schweizerbartsche Vlgsb, p 627
Güldenpfennig M, Loeschke J (1991) Petrographie und Geochemie unterkarbonischer Grauwacken und Vulkanite der Zone von Badenweiler-Lenzkirch und der Umgebung von Präg. Jahreshefte des Geologischen Landesamts Baden-Württemberg 33:5–32
Hancock PL, Barka AA (1987) Kinematic indicators on active normal faults in Western Turkey. J Struct Geol 9(5):573–584
Heidbach O, Reinecker J (2013) Analyse des rezenten Spannungsfelds der Nordschweiz. NAGRA NAB12-05, p 146
Heidbach O, Tingay M, Barth A et al (2008) The World Stress Map database release 2008. doi:10.1594/GFZ.WSM.Rel2008
Heuberger S, Roth P, Zingg O, Naef H, Meier B (2016) The St. Gallen Fault Zone: a long lived, multiphase structure in the North Alpine Foreland Basin revealed by 3D seismic data. Swiss J Geosci 109:83–102
Hinsken S, Ustaszewski K, Wetzel A (2007) Graben width controlling syn-rift sedimentation. The Palaeogene southern Upper Rhine Graben as an example. Int J Earth Sci 96:979–1002
Hofmann F, Schlatter R, Weh M (2000) Blatt 1011 Beggingen (Südhälfte) mit SW-Anteil von Blatt 1012 Singen. Swisstopo, Wabern, p 113
Homberg C, Hu J-C, Angelier J, Bergerat F, Lacombe O (1997) Characterization of stress perturbations near major fault zones: insights from field studies (Jura Mountains) and numerical modelling. J Struct Geol 19(5):703–718
Ibele T (2015) Tectonics of the Hegau and Lake Constance region: a synthesis based on existing literature. Nagra working report, NAB 12–23, Wettingen, p 70
Illies H (1972) The Rhine Graben rift system—plate tectonics and transform faulting. Geophys Surv 1:27–60
Interreg_IIIA (2007) Alpenrhein Bodensee Hochrhein, Projekt "Grenzüberschreitende Bewirtschaftung des Grundwassers im Raum Hegau—Schaffhausen"
Lacombe O, Angelier J, Byrne D et al (1993) Eocene-Oligocene tectonics and kinematics of the Rhine-Saone continental transform zone (eastern France). Tectonics 12:874–888
Laubscher HP (1970) Grundsätzliches zur Tektonik des Rheingrabens. In: Illies H, Mueller S (eds) Graben Problems. Proceedings of an International Rift Symposium held in Karlsruhe 1968, International Upper Mantle Project. Schweitzerbart'sche, Stuttgart,p 79–86
Link K (2010) Die thermo-tektonische Entwicklung des Oberrheingraben-Gebietes seit der Kreide, p 373
Lippolt HJ, Gentner W, Wimmenauer W (1963) Altersbestimmungen nach der Kalium-Argon-Methode an tertiären Eruptivgesteinen Südwestdeutschlands. Jahreshefte des Geologischen Landesamts Baden-Württemberg 6:507–538
Lopes Cardozo GGO, Behrmann JH (2006) Kinematic analysis of the Upper Rhine Graben boundary fault system. J Struct Geol 28(6):1028–1039
Madritsch H (2015) Outcrop-scale fracture systems in the Alpine foreland of central northern Switzerland: kinematics and tectonic context. Swiss J Geosci 108(2):155–181
Madritsch H, Kounov A, Schmid SM et al (2009) Multiple fault reactivations within the intra-continental Rhine-Bresse transfer zone (La Serre Horst, eastern France). Tectonophysics 471(3–4):297–318
Malz A, Madritsch H, Meier B et al (2016) An unusual triangle zone in the external northern Alpine foreland (Switzerland): structural inheritance, kinematics and implications for the development of the adjacent Jura fold-and-thrust belt. Tectonophysics 670:127–143
Marchant R, Ringgenberg Y, Stampfli G et al (2005) Palaeotectonic evolution of the Zürcher Weinland (northern Switzerland) based on 2D and 3D seismic data. Eclogae Geol Helv 98(3):345–362
Marrett R, Allmendinger RW (1990) Kinematic analysis of fault-slip data. J Struct Geol 12(8):973–986
Mazurek M, Hurford AJ, Leu W (2006) Unravelling the multi-stage burial history of the Swiss Molasse Basin: integration of apatite fission track, vitrinite reflectance and biomarker isomerisation analysis. Basin Res 18:27–50
Meier B, Kuhn P, Roth P et al (2014) Tiefenkonvertierung der regionalen Strukturinterpretation der Nagra 2D-Seismik 2011/12. Nagra Working Report, NAB 14-34, Wettingen, p 45
Morris A, Ferrill DA, Henderson DB (1996) Slip-tendency analysis and fault reactivation. Geology 24(3):275–278
Müller WH, Naef H, Graf HR (2002) Geologische Entwicklung der Nordschweiz, Neotektonik und Langzeitszenarien Zürcher Weinland. Nagra Technical Report, NTB 99-08, Wettingen, p 237
Naef H, Birkhäuser P, Roth P (1995) Interpretation der Reflexionsseismik im Gebiet nördlich Lägeren—Zürcher Weinland. NAGRA Technical Report, NTB94-14, Wettingen, p 120
Nagra (2008) Vorschlag geologischer Standortgebiete für das SMA- und das HAA-Lager Geologische Grundlagen, Textband. Nagra Technical Report, NTB08-04, Wettingen, p 439
Ortner H, Reiter F, Acs P (2002) Easy handling of tectonic data: the programs TectonicVB for Mac and TectonicsFP for Windows(TM). Comput Geosci 28(10):1193–1200
Paul W (1948) Beiträge zur Tektonik und Morphologie des mittleren Schwarzwaldes und seiner Ostabdachung. Mitteilungen der Badischen Geologischen Landesanstalt, pp 45–49
Pavoni N (1977) Erdbeben im Gebiet der Schweiz. Eclogae Geol Helv 70:351–370
Pfiffner OA, Erard P, Stäuble M (1997) Two cross sections through the Swiss Molasse Basin (lines E4–E6, W1, W7–W10). In: Pfiffner OA, Lehner P, Heitzmann P et al (eds) Deep Structure of the Swiss Alps: Results of NRP 20. Birkhäuser, Basel, Switzerland, pp 64–72
Rahn MK, Selbekk R (2007) Absolute dating of the youngest sediments of the Swiss Molasse basin by apatite fission track analysis. Swiss J Geosci 100(3):371–381
Regelmann C, Regelmann K (1921) Erläuterungen zur elften Auflage der Geologischen Uebersichtskarte von Württemberg und Badem, dem Elsass. der Pfalz und den weiterhin angrenzenden Gebieten. Württ, Statistisches Landesamt
Reicherter K, Froitzheim N, Jarosinski M et al (2008) Alpine tectonics north of the Alps. In: McCann T (ed) The geology of Central Europe, pp 1233–1285
Reinecker J, Schneider G (2002) Zur Neotektonik der Zollernalb: der Hohenzollerngraben und die Albstadt-Erdbeben. Jahresberichte und Mitteilungen oberrheinischer geologischer Verein 84:391–417
Reiter F, Acs P (1996–2011) Tectonics FP 1.75 Computer Software for Structural Geology. Operating Manual
Rupf I, Nitsch E (2008) Das Geologische Landesmodell von Baden-Würtemberg: Datengrundlage, technische Umsetzung und erste geologische Ergebnisse. Landesamt für Geologie, Rohstoffe und Bergbau Baden-Würtemberg—Informationen 21: p 82
Sawatzki G (2005) Blatt 8215 Ühlingen-Birkendorf. Geologische Karte von Baden-Württemberg 1:25 000, Erläuterungen, p 106
Sawatzki G, Hann HP (2003) Badenweiler-Lenzkirch-Zone (Südschwarzwald). Geologische Karte von Baden-Württemberg 1:50 000, Erläuterungen: p 182

Schaltegger U (2000) U-Pb geochronology of the Southern Black Forest Batholith (Central Variscan Belt): timing of exhumation and granite emplacement. Int J Earth Sci 88:814–828

Schmidle W (1911) Zur Kenntnis der Molasse und der Tektonik am nordwestlichen Bodensee. Zeitschrift der deutschen geologischen Gesellschaft 63(1):522–551

Schmidle W (1918) Die Stratigraphie der Molasse und der Bau des Ueberlinger- und Unterseebeckens. Schriften des Vereins für Gesichte des Bodensees und seiner Umgebung 47:63–83

Schneider G (1979) The Earthquake in the Swabian Jura of 16 November 1911 and present concepts of seismotectonics. Tectonophysics 53:279–288

Schneider G (1993) Beziehungen zwischen Erdbeben und Strukturen der Süddeutschen Grossscholle. Neues Jahrbuch der Geologie und Paleontologie Abhandlungen 189(1–3):275–288

Schreiner A (1989) Blatt 8219 Singen. Geologische Karte von Baden-Württemberg 1:25 000, Erläuterungen, p 139

Schreiner A (1992) Hegau und westlicher Bodensee. Geologische Karte von Baden-Württemberg 1:50 000, Erläuterungen, p 290

Schreiner A (1995) Blatt 8218 Gottmadingen. Geologische Karte von Baden-Württemberg 1:25 000, Erläuterungen, p 142

Schumacher ME (2002) Upper Rhine Graben: role of preexisting structures during rift evolution. Tectonics 21(1):6-1–6-17

Schwarz HU (2012) Das Schwäbisch-Fränkische Bruchmuster. Zeitschrift der Deutschen Gesellschaft für Geowissenschaften 163(4):411–446

Sommaruga A, Eichenberger U, Marillier F (2012) Seismic Atlas of the Swiss Molasse Basin. Swisstopo

Stange S, Brüstle W (2005) The Albstadt/Swabian Jura seismic source zone reviewed through the study of the earthquake of March 22, 2003. Jahresberichte und Mitteilungen oberrheinischer geologischer Verein N.F. 87:391–414

Stange S, Strehlau J (2002) Fault plane solutions of upper and lower crustal earthquakes under the central Molasse basin: evidence of a composite stress field? Conference abstract, 62. Annual Meeting of DGG, March 2002, Hannover

Wallace RE (1951) Geometry of shearing stress and relation to faulting. J Geol 59(2):118–130

Weiskirchner W (1972) Einführung zur Exkursion Hegau. Fortschritte in der Mineralogie, 50, Beiheft 2:70–84

Werner W, Franzke HJ (2001) Postvariszische bis neogene Bruchtektonik und Mineralisation im südlichen Zentralschwarzwald. Zeitschrift der deutschen geologischen Gesellschaft 152(2–4):405–437

Willett SD, Schlunegger F (2010) The last phase of deposition in the Swiss Molasse Basin: from foredeep to negative-alpha basin. Basin Res 22:623–639

Wimmenauer W (1974) The alkaline province of central Europe and France. In: Sorensen H (ed) The Alkaline Rocks. Wiley, London, pp 238–271

Ziegler PA (1992) European Cenozoic rift system. Tectonophysics 208:91–111

Ziegler PA, Dèzes P (2007) Cenozoic uplift of Variscan Massifs in the Alpine foreland: timing and controlling mechanisms. Glob Planet Chang 58(1–4):237–269